Results in Physics 55 (2023) 107118

Contents lists available at ScienceDirect

Results in Physics

journal homepage: www.elsevier.com/locate/rinp

On the fractal-fractional Mittag-Leffler model of a COVID-19 and Zika Co-infection

Shahram Rezapour [a,b,c], Joshua Kiddy K. Asamoah [d], Sina Etemad [b], Ali Akgül [e,f,g,*], İbrahim Avcı [h], Sayed M. El Din [i]

[a] Institute of Research and Development, Duy Tan University, Da Nang 550000, Vietnam
[b] Department of Mathematics, Azarbaijan Shahid Madani University, Tabriz, Iran
[c] Department of Medical Research, China Medical University Hospital, China Medical University, Taichung, Taiwan
[d] Department of Mathematics, Kwame Nkrumah University of Science and Technology, Kumasi, Ghana
[e] Department of Computer Science & Mathematics, Lebanese American University, Beirut, Lebanon
[f] Department of Mathematics, Art and Science Faculty, Siirt University, Siirt 56100, Turkiye
[g] Mathematics Research Center, Department of Mathematics, Near East University, North Cyprus, Mersin 10, Nicosia 99138, Turkiye
[h] Department of Computer Engineering, Faculty of Engineering, Final International University, Kyrenia, Northern Cyprus, via Mersin 10, Turkiye
[i] Center of Research, Faculty of Engineering, Future University in Egypt, New Cairo 11835, Egypt

ARTICLE INFO

Keywords:
COVID-19
Zika virus
Existence
Stability of equilibria
Fractal-fractional derivative
Numerical simulations

ABSTRACT

The World Health Organization declared COVID-19 a global pandemic in March 2020, which had a significant impact on global health and economies. There have been several Zika outbreaks in different regions such as Africa, Southeast Asia, and the Americas. Therefore, it is essential to study the dynamics of these two diseases, taking into account their memory and recurrence effects. A new fractal-fractional hybrid Mittag-Leffler model of COVID-19 and Zika co-dynamics is designed and studied to evaluate the effects of COVID-19 on Zika and vice-versa. The stability analysis of the local asymptotic type at disease-free equilibrium is conducted for the hybrid model. The existence of unique solutions to the model is established via some fixed point results. The fractal-fractional model is proved to be Hyers–Ulam stable. With the help of Newton polynomials, we obtain some numerical algorithms to approximate the solutions of the fractal-fractional hybrid Mittag-Leffler model graphically. The impact of fractional and fractal orders on the dynamics of each of the epidemiological classes is also assessed. In addition, empirical evidence from numerical simulations suggests that implementing measures to contain the transmission of the SARS-CoV-2 virus can significantly contribute to the reduction of co-infections involving the Zika virus. Therefore, it is imperative for healthcare systems to maintain a state of constant vigilance in order to detect any atypical patterns or probable occurrences of co-infections, particularly in areas where both diseases are widespread. Additionally, it is vital to consult the most recent directives provided by health authorities, as our comprehension of diseases may undergo advancements over the course of time.

Introduction

Arbovirus diseases including chikungunya, dengue, zika, transmitted by Aedes aegypti, are one of the most important health concerns publicly in a vast area of tropical and subtropical regions. The Coronavirus pandemic caused by SARS-CoV-2 (the severe acute respiratory syndrome coronavirus 2) has posed more main challenges in territories with overlapping epidemics, raising more demands for health care needs [1]. SARS-CoV-2 and arboviruses (ARBOD) epidemics co-occurrence has become a common concern for health organizations. Both illnesses pose a significant risk of adverse outcomes for either the pregnant woman or the foetus. Existing social and economic gaps increase the risk that susceptible populations will contract Zika virus (ZIKV) and COVID-19. Despite the fact that each disease has distinctive characteristics, there are core concepts behind the identification, communication, and mitigation of infection risk. False information spread via social media platforms has hindered public health activities and patient adoption of recommended mitigating actions. Health care professionals can provide cooperation, social support, and evidence-based information to enhance health-seeking behaviors, thereby reducing risks for pregnant and reproductive-age adults [2]. In 2015 and 2016,

* Corresponding author at: Department of Mathematics, Art and Science Faculty, Siirt University, Siirt 56100, Turkiye.
E-mail addresses: rezapourshahram@yahoo.ca (S. Rezapour), jkkasamoah@knust.edu.gh (J.K.K. Asamoah), sina.etemad@azaruniv.ac.ir (S. Etemad), aliakgul@siirt.edu.tr (A. Akgül), ibrahim.avci@final.edu.tr (İ. Avcı), sayed.eldin22@fue.edu.eg (S.M. El Din).

https://doi.org/10.1016/j.rinp.2023.107118
Received 3 May 2023; Received in revised form 23 October 2023; Accepted 24 October 2023
Available online 3 November 2023

the possibility of ZIKV infection had significant psychological consequences for women who were pregnant or considering pregnancy [3,4]. The virus has the potential to cause neurological harm in foetuses, such as microcephaly, cognitive deficits, and sensory defects. Transmission at a low level of the ZIKV virus continues, and because the virus is endemic, reinfection is unavoidable. Since the majority of infections are asymptomatic, there is concern that transmission may be occurring in the absence of recognized outbreaks, such as the silent and unreported outbreak in Cuba in 2017 and 2018 [5]. The Centers for Disease Control and Prevention state that there are now no active transmission sites in the world (CDC) [6]. The World Health Organization (WHO) has said that ZIKV is a disease that needs more research and development, and that a ZIKV vaccine is needed to treat it [7]. In contrast to the steady progression of ZIKV disease, the World Health Organization (WHO) recorded 528,816,317 confirmed cases of COVID-19 as of 3 June 2022, including 6,294,917 deaths [8]. COVID-19, which is caused by the severe acute respiratory syndrome coronavirus 2 (SARS-CoV-2), was discovered for the first time in December 2019 in Wuhan, China. On March 12, 2020, the WHO declared a global pandemic [2]. SARS-CoV-2, like other coronaviruses, is likely aerosolized for airborne transmission and is conveyed by respiratory droplets [6]. This mode of transmission has necessitated the development of national lockdowns, concealment guidance, and social isolation measures [6]. The arrival of the highly infectious variant viral strains 501.V2 (first identified in South Africa) and B.1.1.7 (discovered in the United Kingdom) raises the need to stop the transmission of this virus. Similar to ZIKV illness, COVID-19 is often asymptomatic, and mild cases might mimic normal rhinorrhea and physiologic dyspnea of pregnancy [6]. Last but not least, ZIKV sickness and the ongoing COVID-19 epidemic have underlined the need for obvious public health concern and a commitment to develop a rigorous mathematical model system to examine the possibilities of co-dynamic transmission. For the sake of the concerns about the spread of various infections, mathematicians provided different mathematical models to discuss and predict dynamics of bacteria–viruses in the progression of diseases. In light of studying the co-dynamics of COVID-19 with other diseases. Omema et al. [9], studied the dynamics of Diabetes and COVID-19. Using data pertinent to the illness dynamics in Lagos, Nigeria, the model is simulated to predict the occurrence of peak periods in the presence or absence of comorbidity. The model is demonstrated to undergo the phenomena of backward bifurcation due to the parameter accounting for greater susceptibility to COVID-19 infection by comorbid susceptibles and the rate of reinfection by individuals who have recovered from a previous COVID-19 infection. In other work, Omame et al. studied COVID-19 and dengue co-infection in Brazil [10]. In the work [11], they presented a fractional-order model for COVID-19 and tuberculosis co-infection using Atangana–Baleanu derivative. Due to their non-local nature, fractional operators have been used in this direction to model phenomena in medicine and engineering. To better understand the subject, we mention several research in which fixed point, and singular and non-singular fractal and/or fractional operators have been utilized. Some of these mathematical models are modeling of mosaic disease [12], Mump virus [13], Hepatitis C [14], anthrax in animals [15], dynamics of environmental persistence of infections [16], canine distemper virus [17], thermostat control [18,19], Navier systems [20,21], pantograph equation [22,23], Ebola disease [24,25], Zika [26], SARS-CoV-2 [27], Meningitis [28], Maize Streak Virus Disease [29], Heartwater transmission dynamics [30], Gonorrhea [31], Monkeypox disease [32,33], Corruption dynamics [34], etc. Moreover, several co-infection models have been studied in the literature by using fractional operators including [35–39]. A new method of differentiation has recently been stated by Atangana et al. [40,41] in which the derivation operator includes two parameters, the first of it is fractal dimension (order) and the second of it is fractional order. In 2019, Atangana and Qureshi predicted and conducted an analysis on the chaos of attractors via fractional-fractal operators (integrals and derivatives) [42]. In 2020, Atangana and Araz derived novel approximations numerically for Chua attractor by using the hybrid fractal-fractional operators [43]. Their book also provides a complete numerical foundation on Lagrange interpolation with respect to variable and non-variable orders. Moreover, Atangana et al. [44] provided a new approximate numerical algorithm in the context of Newton polynomials, which has been utilized for simulating COVID-19 numerically [45]. Asamoah used this method for simulating a fractal-fractional model of Q fever [46]. Also, due to the high accuracy of these new operators in numerical simulation of solutions of various fractal-fractional systems, some mathematicians designed several fractal-fractional models. The outbreak of COVID-19 was simulated in an article done by Shah et al. [47] in Pakistan via fractal-fractional hybrid operators. Gomez-Aguilar et al. [48] provided a new hybrid malaria model via the fractal-fractional derivatives. Ali et al. designed another model of COVID-19 with fractal-fractional derivatives inspired by the real collected numerical data from Wuhan [49]. Najafi et al. [50] designed a Mittag-Leffler hybrid model of fractal-fractional mathematical structure of dynamics of $CD4^+$ T-cells in 2022. Khan et al. [51] extended an existing standard model of tuberculosis to a fractal-fractional model and analyzed it. See other limited articles including [52–54]. Since the notion of fractal-fractional operators is still very new in the literature, it has not yet been applied to study the complicated mathematical structures of co-infections of different diseases. Note that our paper is the first research to study a co-infection in the context of the fractal-fractional model via Mittag-Leffler hybrid kernel. In this study we have contributed in the following ways:

i. We have considered a novel mathematical hybrid model for COVID-19 and Zika, and analyzed via fractal-fractional derivative. To the best of the authors' knowledge, there is no co-infection model using fractal-fractional derivative in the literature.
ii. This model shall be qualitatively analyzed for existence, uniqueness, and stable solutions.
iii. The entire model shall be simulated to examine the effect of COVID-19 on the dynamics of its co-infection with Zika.
iv. The impact and effect of the fractional-fractal derivative on the dynamics of each epidemiological class shall also be examined.

We organize the paper as follows: the fractional operators and fractal-fractional operators are provided in the next section to recall their definitions and properties. Model formulation and its explanations are introduced in Section "Model formulation". We also define all parameters in this section. Section "Analysis of the model" is devoted to analyzing some properties of the model and obtaining the basic reproduction number. In Section "Fractal fractional co-infection model for COVID-19-Zika viruses", we generalize our model to a fractal-fractional hybrid Mittag-Leffler model of co-infection of Zika and COVID-19, and then, in Section "Existence analysis", existence of unique solutions are established. UH-stable solutions are defined and studied in Section "UH-stable solutions". Our approximate numerical algorithms are computed in Section "Numerical scheme via Newton polynomials method" via Newton polynomials. Further, we discuss our simulations in Section "Simulations and discussion" and concludes the paper in Section "Conclusion".

Preliminaries

In this section, we recall and represent several basic notions and notations from fractional and fractal calculus and some known properties required in the sequel.

Definition 1 ([55]). Let $z \in H^1(t_0,t_1), t_1 > t_0, c_1 \in (0,1]$. The c_1^{th}-Atangana–Baleanu derivative in the Caputo sense is given by

$$^{\mathbf{ABC}}D^{c_1}_{t_0,t} z(t) = \frac{\mathbf{AB}(c_1)}{1-c_1}\int_{t_0}^{t} \frac{dz(\mathfrak{q})}{d\mathfrak{q}} E_{c_1}[-\frac{c_1}{1-c_1}(t-\mathfrak{q})^{c_1}]d\mathfrak{q}, \tag{1}$$

where $\mathbf{AB}(c_1)$ satisfying $\mathbf{AB}(0) = \mathbf{AB}(1) = 1$, is a normalization function and $E_{c_1}(\cdot)$ is the Mittag-Leffler function.

Definition 2 ([55]). The c_1^{th}-Atangana–Baleanu integral is defined as

$$ {}^{\mathbf{ABC}}\mathcal{I}^{c_1}_{t_0,t} z(t) = \frac{1-c_1}{\mathbf{AB}(c_1)} z(t) + \frac{c_1}{\mathbf{AB}(c_1)\Gamma(c_1)} \int_{t_0}^{t} z(\mathfrak{q})(t-\mathfrak{q})^{c_1-1} d\mathfrak{q}. \tag{2} $$

Definition 3 ([40]). Let a continuous map $z : (t_0, b) \to [0, \infty)$ be fractal differentiable of dimension c_2. The (c_1, c_2)-fractal-fractional derivative of z of the generalized Mittag-Leffler-type kernel in the Riemann–Liouville sense is given as

$$ {}^{\mathbf{FFML}}\mathcal{D}^{(c_1,c_2)}_{t_0,t} z(t) = \frac{\mathbf{AB}(c_1)}{1-c_1} \frac{\mathrm{d}}{\mathrm{d}t^{c_2}} \int_{t_0}^{t} E_{c_1}\left[-\frac{c_1}{1-c_1}(t-\mathfrak{q})^{c_1}\right] z(\mathfrak{q})\, \mathrm{d}\mathfrak{q}, \quad 0 < c_1, c_2 \le 1, \tag{3} $$

with

$$ \frac{\mathrm{d}z(\mathfrak{q})}{\mathrm{d}\mathfrak{q}^{c_2}} = \lim_{t\to\mathfrak{q}} \frac{z(t)-z(\mathfrak{q})}{t^{c_2}-\mathfrak{q}^{c_2}}, $$

which is the fractal derivative and

$$ \mathbf{AB}(c_1) = 1 - c_1 + \frac{c_1}{\Gamma(c_1)}, $$

and $\mathbf{AB}(0) = \mathbf{AB}(1) = 1$.

Definition 4 ([40]). The (c_1, c_2)-fractal-fractional integral via the Mittag-Leffler-type kernel is defined by

$$ {}^{\mathbf{FFML}}\mathcal{I}^{(c_1,c_2)}_{t_0,t} z(t) = \frac{c_1 c_2}{\Gamma(c_1)\mathbf{AB}(c_1)} \int_{t_0}^{t} \mathfrak{q}^{c_2-1}(t-\mathfrak{q})^{c_1-1} z(\mathfrak{q})\, \mathrm{d}\mathfrak{q} + \frac{(1-c_1)c_2 t^{c_2-1}}{\mathbf{AB}(c_1)} z(t), \tag{4} $$

if the integral is finite-valued, where $c_1, c_2 > 0$.

Model formulation

The saturated incidence rates, which have been utilized in several vector-host disease models [56–59], are used in this paper. The choice is motivated by the fact that the number of effective contacts between susceptible and infectious persons may saturate at high infective levels caused by crowding effect of infectious persons or caused by the precautionary measures put in place by the un-infected individuals. In countries with high co-endemicity of SARS-CoV-2 and arboviruses (Zika virus, as an example), this is the best form of incidence rate. Here, we describe our model. At each time $t \in [0, \tau] := J$, the total population of humans $N^h(t)$ includes several epidemiological states: Susceptible humans $S_h(t)$, infectious humans via COVID-19 $I^h_C(t)$, infectious humans via Zika $I^h_Z(t)$, persons co-infected via COVID-19 and Zika $I^h_{CZ}(t)$. Moreover, symbols $R(t)$ and $I^h_Z(t)$ denote persons who have recovered from COVID-19 and Zika, respectively. At each time t, the total population of vectors $N^v(t)$ includes several states: $S_v(t), I^v_Z(t)$, which denotes susceptible vectors, vectors infected with Zika virus. Susceptible humans get infected via COVID-19 under the rate $\frac{\alpha_C I^h_C}{1+\varphi_1 I^h_C}$. Individuals in this state also acquire Zika either from infected vectors or from infected persons under the rate $\frac{[\alpha_Z I^h_Z + \alpha^h_Z I^v_Z]}{1+\varphi_2 I^h_Z}$. (Human-to-human) transmission of Zika has been established in the literature [60]. Susceptible persons can also get co-infected via both COVID-19 and Zika under the rate $\frac{\alpha_{CZ} I^h_{CZ}}{1+\varphi_3 I^h_{CZ}}$. The constants φ_1, φ_2 and φ_3 adjust the appropriate form of the incidence which determines the rate of new infection. For instance, if $\varphi_1 = 0$, the equivalent incidence is reduced to the mass action or bilinear incidence. However, if $\varphi_1 \neq 0$, then the corresponding incidence becomes a consequence of saturation effects; when the infected number is high, the incidence rate will respond more slowly than linearly to the increase in the corresponding infected compartment. Individuals in this group suffer natural death (just as those in other epidemiological groups) at the rate ϱ_h. The death rates as a result of COVID-19, zika or co-infection are assumed δ_C, δ_Z and δ_{CZ}, respectively. Also, recovery rates from COVID-19, zika virus or co-infection are assumed γ_C, γ_Z and γ_{CZ}, respectively. Humans who have recovered from COVID-19, Zika or co-infection can get re-infected with either COVID-19 or Zika virus at the rates $\vartheta_1 \frac{\alpha_C I^h_C}{1+\varphi_1 I^h_C}$ and $\vartheta_2 \frac{[\alpha_Z I^h_Z + \alpha^h_Z I^v_Z]}{1+\varphi_2 I^h_Z}$, respectively. It is important to state at this point, that the rate of getting re-infection with either COVID-19 or Zika is the same as the rate of incident infection for susceptible individuals. This is also the motivation for the single recovery class in the model, as nothing is known about infection acquired cross-immunity between COVID-19 and zika virus. Recovery from one disease does not give an individual protection against infection with the other disease. Thus, we set $\vartheta_1 = \vartheta_2 = 1$. By considering above assumptions, we can design our fractional model for this co-infection Zika-COVID-19 as

$$ \begin{cases} {}^{\mathbf{ABC}}\mathcal{D}^{c_1}_{0,t} S_h(t) = \Psi^h - \left(\frac{\alpha_C I^h_C}{1+\varphi_1 I^h_C} + \frac{[\alpha_Z I^h_Z + \alpha^h_Z I^v_Z]}{1+\varphi_2 I^h_Z} + \frac{\alpha_{CZ} I^h_{CZ}}{1+\varphi_3 I^h_{CZ}} + \varrho_h \right) S_h, \\ {}^{\mathbf{ABC}}\mathcal{D}^{c_1}_{0,t} I^h_C(t) = \frac{\alpha_C I^h_C}{1+\varphi_1 I^h_C}(S_h + \vartheta_1 R) - \left(\delta_C + \gamma_C + \varrho_h\right) I^h_C - \frac{\zeta_1[\alpha_Z I^h_Z + \alpha^h_Z I^v_Z]}{1+\varphi_2 I^h_Z} I^h_C, \\ {}^{\mathbf{ABC}}\mathcal{D}^{c_1}_{0,t} I^h_Z(t) = \frac{[\alpha_Z I^h_Z + \alpha^h_Z I^v_Z]}{1+\varphi_2 I^h_Z}(S_h + \vartheta_2 R) - \left(\delta_Z + \gamma_Z + \varrho_h\right) I^h_Z - \frac{\zeta_2 \alpha_C I^h_C}{1+\varphi_1 I^h_C} I^h_Z, \\ {}^{\mathbf{ABC}}\mathcal{D}^{c_1}_{0,t} I^h_{CZ}(t) = \frac{\alpha_{CZ} I^h_{CZ}}{1+\varphi_3 I^h_{CZ}} S_h + \frac{\zeta_1[\alpha_Z I^h_Z + \alpha^h_Z I^v_Z]}{1+\varphi_2 I^h_Z} I^h_C + \frac{\zeta_2 \alpha_C I^h_C}{1+\varphi_1 I^h_C} I^h_Z - \left(\delta_{CZ} + \gamma_{CZ} + \varrho_h\right) I^h_{CZ}, \\ {}^{\mathbf{ABC}}\mathcal{D}^{c_1}_{0,t} R(t) = \gamma_C I^h_C + \gamma_Z I^h_Z + \gamma_{CZ} I^h_{CZ} - \left(\varrho_h + \frac{\vartheta_1 \alpha_C I^h_C}{1+\varphi_1 I^h_C} + \frac{\vartheta_2[\alpha_Z I^h_Z + \alpha^h_Z I^v_Z]}{1+\varphi_2 I^h_Z} \right) R, \\ {}^{\mathbf{ABC}}\mathcal{D}^{c_1}_{0,t} S_v(t) = \Psi^v - \left(\frac{\alpha^v_Z (I^h_Z + I^h_{CZ})}{1+\varphi_2 I^h_Z + \varphi_3 I^h_{CZ}} + \varrho_v \right) S_v, \\ {}^{\mathbf{ABC}}\mathcal{D}^{c_1}_{0,t} I^v_Z(t) = \frac{\alpha^v_Z (I^h_Z + I^h_{CZ})}{1+\varphi_2 I^h_Z + \varphi_3 I^h_{CZ}} S_v - \varrho_v I^v_Z, \end{cases} \tag{5} $$

where all parameters are introduced in Table 1.

Analysis of the model

In this part of the research, we shall analyze the co-infection model (5) qualitatively without controls.

Boundedness and positivity

The positivity of the solutions in all time $t > 0$ is one of the most important properties for the given system (5) of the co-infection.

Theorem 1. *The closed set* $\mathcal{K} = \mathcal{K}^h \times \mathcal{K}^v$ *with*

$$ \mathcal{K}^h = \left\{ (S_h, I^h_C, I^h_Z, I^h_{CZ}, R) \in \mathfrak{R}^5_+ : S_h + I^h_C + I^h_Z + I^h_{CZ} + R \le \frac{\Psi^h}{\varrho_h} \right\}, $$

$$ \mathcal{K}^v = \left\{ (S_v, I^v_Z) \in \mathfrak{R}^2_+ : S_v + I^v_Z \le \frac{\Psi^v}{\varrho_v} \right\}, $$

is positively invariant w.r.t the co-infection model (5).

Table 1
All parameters of the hybrid model (5).

	Description
Ψ^h	Human recruitment rate
Ψ^v	Vector recruitment rate
α_C	Effective contact rate for (human-human) transmission of COVID-19
α_Z	Effective contact rate for (human-human) transmission of Zika
α_{CZ}	Effective contact rate for co-infection transmission
α_Z^h	Effective contact rate for (vector-human) transmission of Zika
α_Z^v	Effective contact rate for (human-vector) transmission of Zika
ϱ_h	Human natural death rate
ϱ_v	Vector removal rate
ζ_1, ζ_2	Modification parameter
ϑ_1, ϑ_2	Rate of re-infection with COVID-19 or Zika
$\delta_C, \delta_Z, \delta_{CZ}$	COVID-19, Zika, co-infection disease-induced death rates, respectively
γ_C	COVID-19 recovery rate
γ_Z	Zika recovery rates
γ_{CZ}	COVID-19 recovery rate
$\varphi_1, \varphi_2, \varphi_3$	Parameters accounting for saturating effect

Proof. We add all equations of the co-infection model (5) in relation to the human components and obtain

$$^{ABC}D_{0,t}^{c_1} N^h = \Psi^h - \varrho_h N^h(t) - [\delta_C I_C^h + \delta_Z I_Z^h + \delta_{CZ} I_{CZ}^h]. \tag{6}$$

From (6), we have

$$\Psi^h - (\varrho_h + 3\delta)N^h \leq {}^{ABC}D_{0,t}^{c_1} N^h \leq \Psi^h - \varrho_h N^h,$$

where $\delta = \min\{\delta_C, \delta_Z, \delta_{CZ}\}$. Now, we re-write it as

$$^{ABC}D_{0,t}^{c_1} N^h \leq \Psi^h - \varrho_h N^h. \tag{7}$$

With the help of the comparison theorem for the latter inequality, and by some simplifications, we write

$$N^h(t) \leq \frac{\Psi^h}{\varrho_h}. \tag{8}$$

Hence, for the total population of humans, we have $N^h(t) \leq \frac{\Psi^h}{\varrho_h}$ as $t \to \infty$. The same procedure can be used to show that the total population of vectors is bounded, i.e., $N^v(t) \leq \frac{\Psi^v}{\varrho_v}$. Consequently, the co-infection model (5) admits a solution in $\mathcal{K} = \mathcal{K}^h \times \mathcal{K}^v$, which implies that the given co-infection model is positively invariant. □

The basic reproduction number R_0

The co-infection model (5) admits a DFE (disease-free equilibrium point) whenever we set the right-hand sides of the system to be zero. In this case, DEF point is

$$\psi_0 = \left(S_h^0, I_C^{h0}, I_Z^{h0}, I_{CZ}^{h0}, R^0, S_v^0, I_Z^{v0}\right) = \left(\frac{\Psi^h}{\varrho_h}, 0, 0, 0, 0, \frac{\Psi^v}{\varrho_v}, 0\right).$$

The stability notion for DFE point is derived with the help of a method called the next generation operator [61]. To do this, we write the transfer matrices, respectively, as

$$F = \begin{pmatrix} \alpha_C S_h^0 & 0 & 0 & 0 \\ 0 & \alpha_Z S_h^0 & 0 & \alpha_Z^h S_h^0 \\ 0 & 0 & \alpha_{CZ} S_h^0 & 0 \\ 0 & \alpha_Z^v S_v^0 & \alpha_Z^v S_v^0 & 0 \end{pmatrix}, \quad V = \begin{pmatrix} \mathcal{M}_1 & 0 & 0 & 0 \\ 0 & \mathcal{M}_2 & 0 & 0 \\ 0 & 0 & \mathcal{M}_3 & 0 \\ 0 & 0 & 0 & \varrho_v \end{pmatrix}, \tag{9}$$

where

$$\mathcal{M}_1 = \delta_C + \gamma_C + \varrho_h, \quad \mathcal{M}_2 = \delta_Z + \gamma_Z + \varrho_h, \quad \mathcal{M}_3 = \delta_{CZ} + \gamma_{CZ} + \varrho_h.$$

In this case, the basic reproduction number of the given co-infection model (5) is obtained by

$$R_0 = \rho(FV^{-1}) = \max\{R_{0C}, R_{0Z}, R_{0CZ}\},$$

where R_{0C}, R_{0Z} and R_{0CZ} stand for the corresponding reproduction numbers for COVID-19, Zika and co-infection of both diseases, respectively, and are formulated as

$$R_{0C} = \frac{\alpha_C S_h^0}{\mathcal{M}_1}, \quad R_{0Z} = \frac{1}{2}\frac{\alpha_Z S_h^0}{\mathcal{M}_2} + \frac{1}{2}\sqrt{\left(\frac{\alpha_Z S_h^0}{\mathcal{M}_2}\right)^2 + \frac{4\alpha_Z^h \alpha_Z^v \Psi^h \Psi^v}{\varrho_v^2 \mathcal{M}_2}},$$

$$R_{0CZ} = \frac{\alpha_{CZ} S_h^0}{\mathcal{M}_3}.$$

If we let the corresponding reproduction number of the (human-to-human) Zika transmission and (vector-to-human-to-vector) Zika transmission be $R_{0Z}^h = \frac{\alpha_Z S_h^0}{\mathcal{M}_2}$ and $R_{0Z}^{vh} = \sqrt{\frac{\alpha_Z^h \alpha_Z^v \Psi^h \Psi^v}{\varrho_v^2 \mathcal{M}_2}}$, respectively, then the corresponding reproduction number of Zika can be represented by

$$R_{0Z} = \frac{1}{2}R_{0Z}^h + \frac{1}{2}\sqrt{R_{0Z}^{h2} + 4R_{0Z}^{v2}}.$$

Local asymptotic stability

Theorem 2. *The DFE point, ψ_0, of the given co-infection model (5) of COVID-Zika has the property of the local asymptotic stability if $R_0 < 1$. Otherwise, it is unstable if $R_0 > 1$.*

Proof. To establish the local asymptotic stability for the given co-infection model (5) of COVID-Zika, we analyze the Jacobian matrix of the system (5) computed at the DFE point $\mathcal{H}_0$, and we have

$$\begin{pmatrix} -\varrho_h & -\alpha_C S_h^0 & -\alpha_Z S_h^0 & -\alpha_{CZ} S_h^0 & 0 & 0 & -\alpha_Z^h S_h^0 \\ 0 & \alpha_C S_h^0 - \mathcal{M}_1 & 0 & 0 & 0 & 0 & 0 \\ 0 & 0 & \alpha_Z S_h^0 - \mathcal{M}_2 & 0 & 0 & 0 & \alpha_Z^h \\ 0 & 0 & 0 & \alpha_{CZ} S_h^0 - \mathcal{M}_3 & 0 & 0 & 0 \\ 0 & \gamma_C & \gamma_Z & \gamma_{CZ} & -\varrho_h & 0 & 0 \\ 0 & 0 & -\alpha_Z^v S_v^0 & -\alpha_Z^v S_v^0 & 0 & -\varrho_v & 0 \\ 0 & 0 & \alpha_Z^v S_v^0 & \alpha_Z^v S_v^0 & 0 & 0 & -\varrho_v \end{pmatrix}. \tag{10}$$

The eigenvalues are given by

$$\lambda_1 = -\varrho_v, \quad \lambda_2 = -\varrho_h \quad \text{(with multiplicity of 2)}, \tag{11}$$

and regarding the solutions of three equations

$$\begin{aligned} &(\lambda + \mathcal{M}_1(1 - R_{0C})) = 0, \\ &\lambda^2 + \left(\mathcal{M}_2 + \varrho_v - \alpha_Z S_v^0\right)\lambda + \varrho_v \mathcal{M}_2 (1 - R_{0Z}^h - R_{0Z}^{vh2}) = 0, \\ &(\lambda + \mathcal{M}_3(1 - R_{0CZ})) = 0, \end{aligned} \tag{12}$$

by utilizing the Routh Hurwitz rule, all three Eqs. (12) will admit roots with negative real parts iff $R_{0C} < 1$ and $R_{0Z} < 1$, respectively. In conclusion, the DFE point $\mathcal{H}_0$ admits the property of the local asymptotic stability whenever $R_0 = \max\{R_{0C}, R_{0Z}, R_{0CZ}\} < 1$, and the proof is completed. □

Fractal fractional co-infection model for COVID-19-Zika viruses

In this section, we intend to generalize our model of co-infection Zika-COVID-19 (5) to a fractal-fractional model via the generalized Mittag-Leffler type kernel. We consider all dynamics of transmissions and parameters mentioned in the fractional model (5) and Table 1, and design an extended model with respect to fractal dimension c_2 and

fractional order c_1 as follows

$$\begin{cases} {}^{\mathbf{FFML}}\mathcal{D}^{(c_1,c_2)}_{t_0,t} S_h(t) &= \Psi^h - \left(\dfrac{\alpha_C I^h_C}{1+\varphi_1 I^h_C} \right. \\ &\quad \left. + \dfrac{[\alpha_Z I^h_Z + \alpha^h_Z I^v_Z]}{1+\varphi_2 I^h_Z} + \dfrac{\alpha_{CZ} I^h_{CZ}}{1+\varphi_3 I^h_{CZ}} + \varrho_h \right) S_h, \\ {}^{\mathbf{FFML}}\mathcal{D}^{(c_1,c_2)}_{t_0,t} I^h_C(t) &= \dfrac{\alpha_C I^h_C}{1+\varphi_1 I^h_C}(S_h + \vartheta_1 R) \\ &\quad - \left(\delta_C + \gamma_C + \varrho_h\right) I^h_C - \dfrac{\zeta_1[\alpha_Z I^h_Z + \alpha^h_Z I^v_Z]}{1+\varphi_2 I^h_Z} I^h_C, \\ {}^{\mathbf{FFML}}\mathcal{D}^{(c_1,c_2)}_{t_0,t} I^h_Z(t) &= \dfrac{[\alpha_Z I^h_Z + \alpha^h_Z I^v_Z]}{1+\varphi_2 I^h_Z}(S_h + \vartheta_2 R) - \left(\delta_Z \right. \\ &\quad \left. + \gamma_Z + \varrho_h\right) I^h_Z - \dfrac{\zeta_2 \alpha_C I^h_C}{1+\varphi_1 I^h_C} I^h_Z, \\ {}^{\mathbf{FFML}}\mathcal{D}^{(c_1,c_2)}_{t_0,t} I^h_{CZ}(t) &= \dfrac{\alpha_{CZ} I^h_{CZ}}{1+\varphi_3 I^h_{CZ}} S_h + \dfrac{\zeta_1[\alpha_Z I^h_Z + \alpha^h_Z I^v_Z]}{1+\varphi_2 I^h_Z} I^h_C \\ &\quad + \dfrac{\zeta_2 \alpha_C I^h_C}{1+\varphi_1 I^h_C} I^h_Z - \left(\delta_{CZ} + \gamma_{CZ} + \varrho_h\right) I^h_{CZ}, \\ {}^{\mathbf{FFML}}\mathcal{D}^{(c_1,c_2)}_{t_0,t} R(t) &= \gamma_C I^h_C + \gamma_Z I^h_Z + \gamma_{CZ} I^h_{CZ} \\ &\quad - \left(\varrho_h + \dfrac{\vartheta_1 \alpha_C I^h_C}{1+\varphi_1 I^h_C} + \dfrac{\vartheta_2[\alpha_Z I^h_Z + \alpha^h_Z I^v_Z]}{1+\varphi_2 I^h_Z} \right) R, \\ {}^{\mathbf{FFML}}\mathcal{D}^{(c_1,c_2)}_{t_0,t} S_v(t) &= \Psi^v - \left(\dfrac{\alpha^v_Z (I^h_Z + I^h_{CZ})}{1+\varphi_2 I^h_Z + \varphi_3 I^h_{CZ}} + \varrho_v \right) S_v, \\ {}^{\mathbf{FFML}}\mathcal{D}^{(c_1,c_2)}_{t_0,t} I^v_Z(t) &= \dfrac{\alpha^v_Z (I^h_Z + I^h_{CZ})}{1+\varphi_2 I^h_Z + \varphi_3 I^h_{CZ}} S_v - \varrho_v I^v_Z, \end{cases} \tag{13}$$

for each $t \in [0,\tau] := J$, where ${}^{\mathbf{FFML}}\mathcal{D}^{(c_1,c_2)}_{t_0,t}$ denotes the (c_1,c_2)-fractal-fractional derivative of the Atangana–Baleanu type. In this model, the initial conditions are

$$S_h(0) = S_{h0}, \quad I^h_C(0) = I^h_{C0}, \quad I^h_Z(0) = I^h_{Z0}, \quad I^h_{CZ}(0) = I^h_{CZ0},$$
$$R(0) = R_0, \quad S_v(0) = S_{v0}, \quad I^v_Z(0) = I^v_{Z0},$$

where $S_{h0}, I^h_{C0}, I^h_{Z0}, I^h_{CZ0}, R_0, S_{v0}, I^v_{Z0}$ are nonnegative.

Existence analysis

In the current section, we get help from the well-known theorems of fixed point theory to investigate the existence property. Take the Banach space $\mathcal{X} = \mathbb{F}^7$, by assuming $\mathbb{F} = C(J,\mathbb{R})$ via the norm

$$\|\mathbf{K}\|_{\mathcal{X}} = \|\left(S_h, I^h_C, I^h_Z, I^h_{CZ}, R, S_v, I^v_Z\right)\|_{\mathcal{X}} = \sup\{|P(t)| : \quad t \in J\},$$

for

$$|P| := |S_h| + |I^h_C| + |I^h_Z| + |I^h_{CZ}| + |R| + |S_v| + |I^v_Z|.$$

Further, for the simplicity, the right-hand side of the (c_1,c_2)-fractal-fractional model (13) of the co-infection Zika-COVID-19 can be rewritten as

$$\begin{aligned} \mathbf{X}_1\left(t, S_h(t)\right) &= \Psi^h - \left(\frac{\alpha_C I^h_C}{1+\varphi_1 I^h_C} + \frac{[\alpha_Z I^h_Z + \alpha^h_Z I^v_Z]}{1+\varphi_2 I^h_Z} \right. \\ &\quad \left. + \frac{\alpha_{CZ} I^h_{CZ}}{1+\varphi_3 I^h_{CZ}} + \varrho_h \right) S_h, \\ \mathbf{X}_2\left(t, I^h_C(t)\right) &= \frac{\alpha_C I^h_C}{1+\varphi_1 I^h_C}(S_h + \vartheta_1 R) - \left(\delta_C + \gamma_C + \varrho_h\right) I^h_C \\ &\quad - \frac{\zeta_1[\alpha_Z I^h_Z + \alpha^h_Z I^v_Z]}{1+\varphi_2 I^h_Z} I^h_C, \\ \mathbf{X}_3\left(t, I^h_Z(t)\right) &= \frac{[\alpha_Z I^h_Z + \alpha^h_Z I^v_Z]}{1+\varphi_2 I^h_Z}(S_h + \vartheta_2 R) - \left(\delta_Z + \gamma_Z + \varrho_h\right) I^h_Z \\ &\quad - \frac{\zeta_2 \alpha_C I^h_C}{1+\varphi_1 I^h_C} I^h_Z, \\ \mathbf{X}_4\left(t, I^h_{CZ}(t)\right) &= \frac{\alpha_{CZ} I^h_{CZ}}{1+\varphi_3 I^h_{CZ}} S_h + \frac{[\alpha_Z I^h_Z + \alpha^h_Z I^v_Z]}{1+\varphi_2 I^h_Z} I^h_C \\ &\quad + \frac{\alpha_C I^h_C}{1+\varphi_1 I^h_C} I^h_Z - \left(\delta_{CZ} + \gamma_{CZ} + \varrho_h\right) I^h_{CZ}, \\ \mathbf{X}_5\left(t, R(t)\right) &= \gamma_C I^h_C + \gamma_Z I^h_Z + \gamma_{CZ} I^h_{CZ} \\ &\quad - \left(\varrho_h + \frac{\vartheta_1 \alpha_C I^h_C}{1+\varphi_1 I^h_C} + \frac{\vartheta_2[\alpha_Z I^h_Z + \alpha^h_Z I^v_Z]}{1+\varphi_2 I^h_Z} \right) R, \\ \mathbf{X}_6\left(t, S_v(t)\right) &= \Psi^v - \left(\frac{\alpha^v_Z (I^h_Z + I^h_{CZ})}{1+\varphi_2 I^h_Z + \varphi_3 I^h_{CZ}} + \varrho_v \right) S_v, \\ \mathbf{X}_7\left(t, I^v_Z(t)\right) &= \frac{\alpha^v_Z (I^h_Z + I^h_{CZ})}{1+\varphi_2 I^h_Z + \varphi_3 I^h_{CZ}} S_v - \varrho_v I^v_Z. \end{aligned} \tag{14}$$

Now, the (c_1,c_2)-fractal-fractional model (13) of the co-infection Zika-COVID-19 is reformulated by

$$\begin{cases} {}^{\mathbf{ABR}}\mathcal{D}^{c_1}_{0,t} S_h(t) = c_2 t^{c_2-1} \mathbf{X}_1\left(t, S_h(t)\right), \\ {}^{\mathbf{ABR}}\mathcal{D}^{c_1}_{0,t} I^h_C(t) = c_2 t^{c_2-1} \mathbf{X}_2\left(t, I^h_C(t)\right), \\ {}^{\mathbf{ABR}}\mathcal{D}^{c_1}_{0,t} I^h_Z(t) = c_2 t^{c_2-1} \mathbf{X}_3\left(t, I^h_Z(t)\right), \\ {}^{\mathbf{ABR}}\mathcal{D}^{c_1}_{0,t} I^h_{CZ}(t) = c_2 t^{c_2-1} \mathbf{X}_4\left(t, I^h_{CZ}(t)\right), \\ {}^{\mathbf{ABR}}\mathcal{D}^{c_1}_{0,t} R(t) = c_2 t^{c_2-1} \mathbf{X}_5\left(t, R(t)\right), \\ {}^{\mathbf{ABR}}\mathcal{D}^{c_1}_{0,t} S_v(t) = c_2 t^{c_2-1} \mathbf{X}_6\left(t, S_v(t)\right), \\ {}^{\mathbf{ABR}}\mathcal{D}^{c_1}_{0,t} I^v_Z(t) = c_2 t^{c_2-1} \mathbf{X}_7\left(t, I^v_Z(t)\right). \end{cases} \tag{15}$$

Now, we consider the system (15), and reconstruct the extended mentioned system in the form of the compact initial value problem

$$\begin{cases} {}^{\mathbf{ABR}}\mathcal{D}^{c_1}_{0,s} \mathbf{K}(t) = c_2 t^{c_2-1} \mathbf{X}\left(t, \mathbf{K}(t)\right), \\ \mathbf{K}(0) = \mathbf{K}_0, \end{cases} \tag{16}$$

by assuming

$$\begin{aligned} \mathbf{K}(t) &= \left(S_h(t), I^h_C(t), I^h_Z(t), I^h_{CZ}(t), R(t), S_v(t), I^v_Z(t)\right)^T, \\ \mathbf{K}_0 &= \left(S_{h0}, I^h_{C0}, I^h_{Z0}, I^h_{CZ0}, R_0, S_{v0}, I^v_{Z0}\right)^T, \quad c_1, c_2 \in (0,1], \end{aligned} \tag{17}$$

and

$$\mathbf{X}\left(t, \mathbf{K}(t)\right) = \begin{cases} \mathbf{X}_1\left(t, S_h(t)\right), \\ \mathbf{X}_2\left(t, I^h_C(t)\right), \\ \mathbf{X}_3\left(t, I^h_Z(t)\right), \\ \mathbf{X}_4\left(t, I^h_{CZ}(t)\right), \\ \mathbf{X}_5\left(t, R(t)\right), \\ \mathbf{X}_6\left(t, S_v(t)\right), \\ \mathbf{X}_7\left(t, I^v_Z(t)\right), \quad t \in J. \end{cases} \tag{18}$$

Definition of the non-singular fractional ABR-derivative gives (16) as

$$\frac{\mathbf{AB}(c_1)}{1-c_1} \frac{\mathrm{d}}{\mathrm{d}t} \int_0^t E_{c_1}\left[-\frac{c_1}{1-c_1}(t-\mathfrak{q})^{c_1}\right] \mathbf{K}(\mathfrak{q})\,\mathrm{d}\mathfrak{q} = c_2 t^{c_2-1} \mathbf{X}\left(t, \mathbf{K}(t)\right). \tag{19}$$

Moreover, taking the fractal-fractional Atangana–Baleanu integral on (19), it yields

$$\begin{aligned} \mathbf{K}(t) &= \mathbf{K}(0) + \frac{(1-c_1) c_2 t^{c_2-1}}{\mathbf{AB}(c_1)} \mathbf{X}(t, \mathbf{K}(t)) \\ &\quad + \frac{c_1 c_2}{\Gamma(c_1)\mathbf{AB}(c_1)} \int_0^t \mathfrak{q}^{c_2-1} (t-\mathfrak{q})^{c_1-1} \mathbf{X}(\mathfrak{q}, \mathbf{K}(\mathfrak{q}))\,\mathrm{d}\mathfrak{q}. \end{aligned} \tag{20}$$

By considering the above basic fractal-fractional integral equation, we obtain the following extended system of fractal-fractional integral

equations as

$$
\begin{aligned}
S_h(t) &= S_{h0} + \frac{(1-c_1)c_2t^{c_2-1}}{\mathbf{AB}(c_1)}\mathbf{X}_1(t,S_h(t)) \\
&\quad + \frac{c_1c_2}{\Gamma(c_1)\mathbf{AB}(c_1)}\int_0^t \mathrm{q}^{c_2-1}(t-\mathrm{q})^{c_1-1}\mathbf{X}_1(\mathrm{q},S_h(\mathrm{q}))\,\mathrm{dq},\\
I_C^h(t) &= I_{C0}^h + \frac{(1-c_1)c_2t^{c_2-1}}{\mathbf{AB}(c_1)}\mathbf{X}_2(t,I_C^h(t)) \\
&\quad + \frac{c_1c_2}{\Gamma(c_1)\mathbf{AB}(c_1)}\int_0^t \mathrm{q}^{c_2-1}(t-\mathrm{q})^{c_1-1}\mathbf{X}_2(\mathrm{q},I_C^h(\mathrm{q}))\,\mathrm{dq},\\
I_Z^h(t) &= I_{Z0}^h + \frac{(1-c_1)c_2t^{c_2-1}}{\mathbf{AB}(c_1)}\mathbf{X}_3(t,I_Z^h(t)) \\
&\quad + \frac{c_1c_2}{\Gamma(c_1)\mathbf{AB}(c_1)}\int_0^t \mathrm{q}^{c_2-1}(t-\mathrm{q})^{c_1-1}\mathbf{X}_3(\mathrm{q},I_Z^h(\mathrm{q}))\,\mathrm{dq},\\
I_{CZ}^h(t) &= I_{CZ0}^h + \frac{(1-c_1)c_2t^{c_2-1}}{\mathbf{AB}(c_1)}\mathbf{X}_4(t,I_{CZ}^h(t)) \\
&\quad + \frac{c_1c_2}{\Gamma(c_1)\mathbf{AB}(c_1)}\int_0^t \mathrm{q}^{c_2-1}(t-\mathrm{q})^{c_1-1}\mathbf{X}_4(\mathrm{q},I_{CZ}^h(\mathrm{q}))\,\mathrm{dq},\\
R(t) &= R_0 + \frac{(1-c_1)c_2t^{c_2-1}}{\mathbf{AB}(c_1)}\mathbf{X}_5(t,R(t)) \\
&\quad + \frac{c_1c_2}{\Gamma(c_1)\mathbf{AB}(c_1)}\int_0^t \mathrm{q}^{c_2-1}(t-\mathrm{q})^{c_1-1}\mathbf{X}_5(\mathrm{q},R(\mathrm{q}))\,\mathrm{dq},\\
S_v(t) &= S_{v0} + \frac{(1-c_1)c_2t^{c_2-1}}{\mathbf{AB}(c_1)}\mathbf{X}_6(t,S_v(t)) \\
&\quad + \frac{c_1c_2}{\Gamma(c_1)\mathbf{AB}(c_1)}\int_0^t \mathrm{q}^{c_2-1}(t-\mathrm{q})^{c_1-1}\mathbf{X}_6(\mathrm{q},S_v(\mathrm{q}))\,\mathrm{dq},\\
I_Z^v(t) &= I_{Z0}^v + \frac{(1-c_1)c_2t^{c_2-1}}{\mathbf{AB}(c_1)}\mathbf{X}_7(t,I_Z^v(t)) \\
&\quad + \frac{c_1c_2}{\Gamma(c_1)\mathbf{AB}(c_1)}\int_0^t \mathrm{q}^{c_2-1}(t-\mathrm{q})^{c_1-1}\mathbf{X}_7(\mathrm{q},I_Z^v(\mathrm{q}))\,\mathrm{dq}.
\end{aligned}
$$

We regard a new map to investigate a fixed-point problem, by giving $T : \mathcal{X} \to \mathcal{X}$ as

$$
\begin{aligned}
T(\mathbf{K}(t)) &= \mathbf{K}(0) + \frac{(1-c_1)c_2t^{c_2-1}}{\mathbf{AB}(c_1)}\mathbf{X}(t,\mathbf{K}(t)) \\
&\quad + \frac{c_1c_2}{\Gamma(c_1)\mathbf{AB}(c_1)}\int_0^t \mathrm{q}^{c_2-1}(t-\mathrm{q})^{c_1-1}\mathbf{X}(\mathrm{q},\mathbf{K}(\mathrm{q}))\,\mathrm{dq}. \qquad (21)
\end{aligned}
$$

In relation to the existence property of solution on the (c_1, c_2)-fractal-fractional model (13) of the co-infection Zika-COVID-19, we use the following:

Theorem 3 (*[62] Leray–Schauder theorem*). *Let $\mathcal{X}$ be a Banach space, $U \subset \mathcal{X}$ a convex closed bounded set, $\mathbb{G} \subset U$ an open set, and $0 \in \mathbb{G}$. Then for the continuous and compact map $T : \bar{\mathbb{G}} \to U$, either:*

(HY1) $\exists\, x \in \bar{\mathbb{G}}$ *s.t.* $x = T(x)$, *or*
(HY2) $\exists\, x \in \partial\mathbb{G}$ *and* $0 < \mu < 1$ *s.t.* $x = \mu T(x)$.

Theorem 4. *Let $\mathbf{X} \in C(J \times \mathcal{X}, \mathcal{X})$, and also assume:*

(G1) $\exists\, \mathcal{F} \in L^1(J, \mathbb{R}^+)$ *and* $\exists\, Y \in C([0,\infty),(0,\infty))$ *(Y is non-decreasing) s.t.* $\forall\, t \in J$ *and* $\mathbf{K} \in \mathcal{X}$,

$$\Big|\mathbf{X}(t,\mathbf{K}(t))\Big| \le \mathcal{F}(t)Y(|\mathbf{K}(t)|);$$

(G2) $\exists\, \Re > 0$ *s.t.*

$$\frac{\Re}{\Big[\frac{(1-c_1)c_2\tau^{c_2-1}}{\mathbf{AB}(c_1)} + \frac{c_1c_2\tau^{c_1+c_2-1}\Gamma(c_2)}{\Gamma(c_1+c_2)\mathbf{AB}(c_1)}\Big]\mathcal{F}_0^*Y(\Re) + \mathbf{K}_0} > 1, \qquad (22)$$

with $\mathcal{F}_0^* = \sup_{t\in J}|\mathcal{F}(t)|$.

Then for the fractal-fractional problem (16) and so, for the (c_1, c_2)-fractal-fractional model (13) of the co-infection Zika-COVID-19, at least a solution exists on J.

Proof. To start our argument, consider $T : \mathcal{X} \to \mathcal{X}$ given by (21) and

$$N_R = \Big\{\mathbf{K} \in \mathcal{X} \;:\; \|\mathbf{K}\|_{\mathcal{X}} \le R\Big\}, \quad \text{for some } R > 0.$$

Evidently, the continuity of $\mathbf{X}$ implies that of the operator T. Now (G1) gives the following estimate

$$
\begin{aligned}
\Big|T(\mathbf{K}(t))\Big| &\le \Big|\mathbf{K}(0)\Big| + \frac{(1-c_1)c_2t^{c_2-1}}{\mathbf{AB}(c_1)}\Big|\mathbf{X}(t,\mathbf{K}(t))\Big| \\
&\quad + \frac{c_1c_2}{\Gamma(c_1)\mathbf{AB}(c_1)}\int_0^t \mathrm{q}^{c_2-1}(t-\mathrm{q})^{c_1-1}\Big|\mathbf{X}(\mathrm{q},\mathbf{K}(\mathrm{q}))\Big|\,\mathrm{dq} \\
&\le \mathbf{K}_0 + \frac{(1-c_1)c_2t^{c_2-1}}{\mathbf{AB}(c_1)}\mathcal{F}(t)Y(|\mathbf{K}(t)|) \\
&\quad + \frac{c_1c_2}{\Gamma(c_1)\mathbf{AB}(c_1)}\int_0^t \mathrm{q}^{c_2-1}(t-\mathrm{q})^{c_1-1}\mathcal{F}(\mathrm{q})Y(|\mathbf{K}(\mathrm{q})|)\,\mathrm{dq} \\
&\le \mathbf{K}_0 + \frac{(1-c_1)c_2\tau^{c_2-1}}{\mathbf{AB}(c_1)}\mathcal{F}_0^*Y(R) + \frac{c_1c_2\tau^{c_1+c_2-1}B(c_1,c_2)}{\Gamma(c_1)\mathbf{AB}(c_1)}\mathcal{F}_0^*Y(R) \\
&= \mathbf{K}_0 + \frac{(1-c_1)c_2\tau^{c_2-1}}{\mathbf{AB}(c_1)}\mathcal{F}_0^*Y(R) + \frac{c_1c_2\tau^{c_1+c_2-1}\Gamma(c_2)}{\mathbf{AB}(c_1)\Gamma(c_1+c_2)}\mathcal{F}_0^*Y(R),
\end{aligned}
$$

for $\mathbf{K} \in N_R$. We get

$$\|T\mathbf{K}\|_{\mathbb{X}} \le \mathbf{K}_0 + \Big[\frac{(1-c_1)c_2\tau^{c_2-1}}{\mathbf{AB}(c_1)} + \frac{c_1c_2\tau^{c_1+c_2-1}\Gamma(c_2)}{\mathbf{AB}(c_1)\Gamma(c_1+c_2)}\Big]\mathcal{F}_0^*Y(R) < \infty. \qquad (23)$$

So $\|T\mathbf{K}\|_{\mathbb{X}} < \infty$ and T is uniformly bounded on $\mathcal{X}$. In the following, choose $t, z \in [0,\tau] := J$ arbitrarily with $t < z$ and $\mathbf{K} \in N_R$. Take

$$\sup_{(t,\mathbf{K})\in J\times N_R}|\mathbf{X}(t,\mathbf{K}(t))| = \mathbf{X}^* < \infty.$$

Then

$$
\begin{aligned}
\Big|T(\mathbf{K}(z)) - T(\mathbf{K}(t))\Big| &\le \Big|\frac{(1-c_1)c_2z^{c_2-1}}{\mathbf{AB}(c_1)}\mathbf{X}(z,\mathbf{K}(z)) \\
&\quad - \frac{(1-c_1)c_2t^{c_2-1}}{\mathbf{AB}(c_1)}\mathbf{X}(t,\mathbf{K}(t)) \\
&\quad + \frac{c_1c_2}{\Gamma(c_1)\mathbf{AB}(c_1)}\int_0^z \mathrm{q}^{c_2-1}(z-\mathrm{q})^{c_1-1}\mathbf{X}(\mathrm{q},\mathbf{K}(\mathrm{q}))\,\mathrm{dq} \\
&\quad - \frac{c_1c_2}{\Gamma(c_1)\mathbf{AB}(c_1)}\int_0^t \mathrm{q}^{c_2-1}(t-\mathrm{q})^{c_1-1}\mathbf{X}(\mathrm{q},\mathbf{K}(\mathrm{q}))\,\mathrm{dq}\Big| \\
&\le \frac{(1-c_1)c_2\mathbf{X}^*}{\mathbf{AB}(c_1)}(z^{c_2-1} - t^{c_2-1}) \qquad (24) \\
&\quad + \frac{c_1c_2\mathbf{X}^*}{\Gamma(c_1)\mathbf{AB}(c_1)}\Big|\int_0^z \mathrm{q}^{c_2-1}(z-\mathrm{q})^{c_1-1}\,\mathrm{dq} \\
&\quad - \int_0^t \mathrm{q}^{c_2-1}(t-\mathrm{q})^{c_1-1}\,\mathrm{dq}\Big| \\
&\le \frac{(1-c_1)c_2\mathbf{X}^*}{\mathbf{AB}(c_1)}(z^{c_2-1} - t^{c_2-1}) \\
&\quad + \frac{c_1c_2\mathbf{X}^*B(c_1,c_2)}{\Gamma(c_1)\mathbf{AB}(c_1)}\big[z^{c_1+c_2-1} - t^{c_1+c_2-1}\big] \\
&= \frac{(1-c_1)c_2\mathbf{X}^*}{\mathbf{AB}(c_1)}(z^{c_2-1} - t^{c_2-1}) \\
&\quad + \frac{c_1c_2\mathbf{X}^*\Gamma(c_2)}{\Gamma(c_1+c_2)\mathbf{AB}(c_1)}\big[z^{c_1+c_2-1} - t^{c_1+c_2-1}\big],
\end{aligned}
$$

where (independent of $\mathbf{K}$) (24) tends to 0 as $z \to t$. Therefore,

$$\lim_{z\to t}\|T(\mathbf{K}(z)) - T(\mathbf{K}(t))\|_{\mathcal{X}} = 0,$$

and T is equicontinuous, and so it is compact on N_R by referring to the Arzelá–Ascoli theorem. Since all the conditions of Theorem 3 to be held on T, thus one of (HY1) or (HY2) will be valid. From (G2), set

$$\Phi := \Big\{\mathbf{K} \in \mathcal{X} \;:\; \|\mathbf{K}\|_{\mathcal{X}} < \Re\Big\},$$

for some $\Re > 0$ via $\mathbf{K}_0 + \Big[\frac{(1-c_1)c_2\tau^{c_2-1}}{\mathbf{AB}(c_1)} + \frac{c_1c_2\tau^{c_1+c_2-1}\Gamma(c_2)}{\Gamma(c_1+c_2)\mathbf{AB}(c_1)}\Big]\mathcal{F}_0^*Y(\Re) < \Re$. With the help of (G1) and by (23), we estimate

$$\|T\mathbf{K}\|_{\mathcal{X}} \le \mathbf{K}_0 + \Big[\frac{(1-c_1)c_2\tau^{c_2-1}}{\mathbf{AB}(c_1)} + \frac{c_1c_2\tau^{c_1+c_2-1}\Gamma(c_2)}{\Gamma(c_1+c_2)\mathbf{AB}(c_1)}\Big]\mathcal{F}_0^*Y(\|\mathbf{K}\|_{\mathcal{X}}). \qquad (25)$$

Next, we consider the existence of $\mathbf{K} \in \partial\Phi$ and $0 < \mu < 1$ with $\mathbf{K} = \mu T(\mathbf{K})$. For these selections of $\mathbf{K}$ and μ, and by (25),

$$\begin{aligned}\Re &= \|\mathbf{K}\|_{\mathcal{X}} = \mu\|T\mathbf{K}\|_{\mathcal{X}}\\ &< \mathbf{K}_0 + \left[\frac{(1-c_1)c_2\tau^{c_2-1}}{\mathbf{AB}(c_1)} + \frac{c_1c_2\tau^{c_1+c_2-1}\Gamma(c_2)}{\Gamma(c_1+c_2)\mathbf{AB}(c_1)}\right]\mathcal{F}_0^* Y(\|\mathbf{K}\|_{\mathcal{X}})\\ &< \mathbf{K}_0 + \left[\frac{(1-c_1)c_2\tau^{c_2-1}}{\mathbf{AB}(c_1)} + \frac{c_1c_2\tau^{c_1+c_2-1}\Gamma(c_2)}{\Gamma(c_1+c_2)\mathbf{AB}(c_1)}\right]\mathcal{F}_0^* Y(\Re) < \Re,\end{aligned}$$

which is impossible. Therefore, (HY2) does not satisfy and T possesses a fixed–point in $\bar{\Phi}$ by Theorem 3 which is the same solution of the (c_1, c_2)-fractal-fractional model (13) of the co-infection Zika-COVID-19. □

To prove the uniqueness of solution of the (c_1, c_2)-fractal-fractional model (13) of the co-infection Zika-COVID-19, we investigate the Lipschitz property for the kernels $\mathbf{X}_j$, $(j = 1, \dots, 7)$ considered in (14).

Lemma 1. *Let $S_h, I_C^h, I_Z^h, I_{CZ}^h, R, S_v, I_Z^v, S_h^*, I_C^{h*}, I_Z^{h*}, I_{CZ}^{h*}, R^*, S_v^*, I_Z^{v*} \in \mathbb{F} := C(J, \mathbb{R})$, and for all $t \in J$, $1 + \varphi_2 I_Z^h(t) > I_Z^v(t)$, $1 + \varphi_2 I_Z^{h*}(t) > I_Z^v(t)$, and*

(G3) $\exists\, \varkappa_1, \varkappa_2, \varkappa_3, \varkappa_4, \varkappa_5, \varkappa_6, \varkappa_7 > 0$ s.t. $\|S_h\| \le \varkappa_1$, $\|I_C^h\| \le \varkappa_2$, $\|I_Z^h\| \le \varkappa_3$, $\|I_{CZ}^h\| \le \varkappa_4$, $\|R\| \le \varkappa_5$, $\|S_v\| \le \varkappa_6$ and $\|I_Z^v\| \le \varkappa_7$.

Then $\mathbf{X}_1, \mathbf{X}_2, \mathbf{X}_3, \mathbf{X}_4, \mathbf{X}_5, \mathbf{X}_6, \mathbf{X}_7$ defined by (14) are Lipschitz with $L_1, L_2, L_3, L_4, L_5, L_6, L_7 > 0$, where

$$\begin{aligned}L_1 &= \alpha_C\varkappa_2 + \alpha_Z\varkappa_3 + \alpha_Z^h\varkappa_7 + \alpha_{CZ}\varkappa_4 + \varrho_h > 0,\\ L_2 &= \alpha_C(\varkappa_1 + \vartheta_1\varkappa_5) + (\delta_C + \gamma_C + \varrho_h) + \zeta_1(\alpha_Z\varkappa_3 + \alpha_Z^h\varkappa_7) > 0,\\ L_3 &= (\alpha_Z + \alpha_Z^h)(\varkappa_1 + \vartheta_2\varkappa_5) + (\delta_Z + \gamma_Z + \varrho_h) + \zeta_2\alpha_C\varkappa_2 > 0,\\ L_4 &= \alpha_{CZ}\varkappa_1 + (\delta_{CZ} + \gamma_{CZ} + \varrho_h) > 0,\\ L_5 &= \varrho_h + \vartheta_1\alpha_C\varkappa_2 + \vartheta_2\alpha_Z\varkappa_3 + \vartheta_2\alpha_Z^h\varkappa_7 > 0,\\ L_6 &= \alpha_Z^v\varkappa_3 + \alpha_Z^v\varkappa_4 + \varrho_v > 0, \qquad L_7 = \varrho_v > 0.\end{aligned} \tag{26}$$

Proof. For the function $\mathbf{X}_1$, we choose $S_h, S_h^* \in \mathbb{F} := C(J, \mathbb{R})$ arbitrarily. Then

$$\begin{aligned}&\|\mathbf{X}_1(t, S_h(t)) - \mathbf{X}_1(t, S_h^*(t))\|\\ &\quad= \Big\| \Big[\Psi^h - \left(\frac{\alpha_C I_C^h}{1+\varphi_1 I_C^h} + \frac{[\alpha_Z I_Z^h + \alpha_Z^h I_Z^v]}{1+\varphi_2 I_Z^h} + \frac{\alpha_{CZ} I_{CZ}^h}{1+\varphi_3 I_{CZ}^h} + \varrho_h\right) S_h \Big]\\ &\quad- \Big[\Psi^h - \left(\frac{\alpha_C I_C^h}{1+\varphi_1 I_C^h} + \frac{[\alpha_Z I_Z^h + \alpha_Z^h I_Z^v]}{1+\varphi_2 I_Z^h} + \frac{\alpha_{CZ} I_{CZ}^h}{1+\varphi_3 I_{CZ}^h} + \varrho_h\right) S_h^* \Big] \Big\|\\ &\quad\le \Big\| \Big[\frac{\alpha_C I_C^h}{1+\varphi_1 I_C^h} + \frac{[\alpha_Z I_Z^h + \alpha_Z^h I_Z^v]}{1+\varphi_2 I_Z^h} + \frac{\alpha_{CZ} I_{CZ}^h}{1+\varphi_3 I_{CZ}^h} + \varrho_h \Big] \big(S_h(t) - S_h^*(t)\big) \Big\|\\ &\quad\le \big[\alpha_C\|I_C^h\| + \alpha_Z\|I_Z^h\| + \alpha_Z^h\|I_Z^v\| + \alpha_{CZ}\|I_{CZ}^h\| + \varrho_h\big]\|S_h(t) - S_h^*(t)\|\\ &\quad\le \big[\alpha_C\varkappa_2 + \alpha_Z\varkappa_3 + \alpha_Z^h\varkappa_7 + \alpha_{CZ}\varkappa_4 + \varrho_h\big]\|S_h(t) - S_h^*(t)\|\\ &\quad= L_1\|S_h(t) - S_h^*(t)\|.\end{aligned}$$

This shows that $\mathbf{X}_1$ is Lipschitz w.r.t. S_h with constant $L_1 > 0$.

For the function $\mathbf{X}_2$, we choose $I_C^h, I_C^{h*} \in \mathbb{F} := C(J, \mathbb{R})$ arbitrarily. Then

$$\begin{aligned}&\|\mathbf{X}_2(t, I_C^h(t)) - \mathbf{X}_2(t, I_C^{h*}(t))\|\\ &\quad= \Big\| \Big[\frac{\alpha_C I_C^h}{1+\varphi_1 I_C^h}(S_h + \vartheta_1 R) - \big(\delta_C + \gamma_C + \varrho_h\big) I_C^h\\ &\quad- \frac{\zeta_1[\alpha_Z I_Z^h + \alpha_Z^h I_Z^v]}{1+\varphi_2 I_Z^h} I_C^h \Big]\\ &\quad- \Big[\frac{\alpha_C I_C^{h*}}{1+\varphi_1 I_C^{h*}}(S_h + \vartheta_1 R) - \big(\delta_C + \gamma_C + \varrho_h\big) I_C^{h*}\\ &\quad- \frac{\zeta_1[\alpha_Z I_Z^h + \alpha_Z^h I_Z^v]}{1+\varphi_2 I_Z^h} I_C^{h*} \Big] \Big\|\\ &\quad\le \big[\alpha_C(S_h + \vartheta_1 R) + (\delta_C + \gamma_C + \varrho_h)\\ &\quad+ \zeta_1(\alpha_Z I_Z^h + \alpha_Z^h I_Z^v) \big] \|I_C^h(t) - I_C^{h*}(t)\|\\ &\quad\le \big[\alpha_C(\|S_h\| + \vartheta_1\|R\|) + (\delta_C + \gamma_C + \varrho_h)\\ &\quad+ \zeta_1(\alpha_Z\|I_Z^h\| + \alpha_Z^h\|I_Z^v\|) \big] \|I_C^h(t) - I_C^{h*}(t)\|\\ &\quad\le \big[\alpha_C(\varkappa_1 + \vartheta_1\varkappa_5) + (\delta_C + \gamma_C + \varrho_h)\\ &\quad+ \zeta_1(\alpha_Z\varkappa_3 + \alpha_Z^h\varkappa_7) \big] \|I_C^h(t) - I_C^{h*}(t)\|\\ &\quad= L_2\|I_C^h(t) - I_C^{h*}(t)\|.\end{aligned}$$

This shows that $\mathbf{X}_2$ is Lipschitz w.r.t. I_C^h with constant $L_2 > 0$.

For $\mathbf{X}_3$, we choose $I_Z^h, I_Z^{h*} \in \mathbb{F} := C(J, \mathbb{R})$ arbitrarily. Then

$$\begin{aligned}&\|\mathbf{X}_3(t, I_Z^h(t)) - \mathbf{X}_3(t, I_Z^{h*}(t))\|\\ &\quad= \Big\| \Big[\frac{[\alpha_Z I_Z^h + \alpha_Z^h I_Z^v]}{1+\varphi_2 I_Z^h}(S_h + \vartheta_2 R)\\ &\quad- \big(\delta_Z + \gamma_Z + \varrho_h\big) I_Z^h - \frac{\zeta_2\alpha_C I_C^h}{1+\varphi_1 I_C^h} I_Z^h \Big]\\ &\quad- \Big[\frac{[\alpha_Z I_Z^{h*} + \alpha_Z^h I_Z^v]}{1+\varphi_2 I_Z^{h*}}(S_h + \vartheta_2 R)\\ &\quad- \big(\delta_Z + \gamma_Z + \varrho_h\big) I_Z^{h*} - \frac{\zeta_2\alpha_C I_C^h}{1+\varphi_1 I_C^h} I_Z^{h*} \Big] \Big\|\\ &\quad\le \big[(\alpha_Z + \alpha_Z^h)(S_h + \vartheta_2 R) + (\delta_Z + \gamma_Z + \varrho_h)\\ &\quad+ \zeta_2\alpha_C I_C^h \big] \|I_Z^h(t) - I_Z^{h*}(t)\|\\ &\quad\le \big[(\alpha_Z + \alpha_Z^h)(\|S_h\| + \vartheta_2\|R\|) + (\delta_Z + \gamma_Z + \varrho_h)\\ &\quad+ \zeta_2\alpha_C\|I_C^h\| \big] \|I_Z^h(t) - I_Z^{h*}(t)\|\\ &\quad\le \big[(\alpha_Z + \alpha_Z^h)(\varkappa_1 + \vartheta_2\varkappa_5) + (\delta_Z + \gamma_Z + \varrho_h)\\ &\quad+ \zeta_2\alpha_C\varkappa_2 \big] \|I_Z^h(t) - I_Z^{h*}(t)\|\\ &\quad= L_3\|I_Z^h(t) - I_Z^{h*}(t)\|.\end{aligned}$$

This shows that $\mathbf{X}_3$ is Lipschitz w.r.t. I_Z^h with constant $L_3 > 0$.

For $\mathbf{X}_4$, we choose $I_{CZ}^h, I_{CZ}^{h*} \in \mathbb{F} := C(J, \mathbb{R})$ arbitrarily. Then

$$\begin{aligned}&\|\mathbf{X}_4(t, I_{CZ}^h(t)) - \mathbf{X}_4(t, I_{CZ}^{h*}(t))\|\\ &\quad= \Big\| \Big[\frac{\alpha_{CZ} I_{CZ}^h}{1+\varphi_3 I_{CZ}^h} S_h + \frac{\zeta_1[\alpha_Z I_Z^h + \alpha_Z^h I_Z^v]}{1+\varphi_2 I_Z^h} I_C^h + \frac{\zeta_2\alpha_C I_C^h}{1+\varphi_1 I_C^h} I_Z^h\\ &\quad- \big(\delta_{CZ} + \gamma_{CZ} + \varrho_h\big) I_{CZ}^h \Big]\\ &\quad- \Big[\frac{\alpha_{CZ} I_{CZ}^{h*}}{1+\varphi_3 I_{CZ}^{h*}} S_h + \frac{\zeta_1[\alpha_Z I_Z^h + \alpha_Z^h I_Z^v]}{1+\varphi_2 I_Z^h} I_C^h + \frac{\zeta_2\alpha_C I_C^h}{1+\varphi_1 I_C^h} I_Z^h\\ &\quad- (\delta_{CZ} + \gamma_{CZ} + \varrho_h) I_{CZ}^{h*} \Big] \Big\|\\ &\quad\le \big[\alpha_{CZ} S_h + (\delta_{CZ} + \gamma_{CZ} + \varrho_h)\big]\|I_{CZ}^h(t) - I_{CZ}^{h*}(t)\|\\ &\quad\le \big[\alpha_{CZ}\|S_h\| + (\delta_{CZ} + \gamma_{CZ} + \varrho_h)\big]\|I_{CZ}^h(t) - I_{CZ}^{h*}(t)\|\\ &\quad\le \big[\alpha_{CZ}\varkappa_1 + (\delta_{CZ} + \gamma_{CZ} + \varrho_h)\big]\|I_{CZ}^h(t) - I_{CZ}^{h*}(t)\|\\ &\quad= L_4\|I_{CZ}^h(t) - I_{CZ}^{h*}(t)\|.\end{aligned}$$

This shows that $\mathbf{X}_4$ is Lipschitz w.r.t. I_{CZ}^h with constant $L_4 > 0$.

For $\mathbf{X}_5$, we choose $R, R^* \in \mathbb{F} := C(J, \mathbb{R})$ arbitrarily. Then

$$\begin{aligned}&\|\mathbf{X}_5(t, R(t)) - \mathbf{X}_5(t, R^*(t))\|\\ &\quad= \Big\| \Big[\gamma_C I_C^h + \gamma_Z I_Z^h + \gamma_{CZ} I_{CZ}^h\\ &\quad- \left(\varrho_h + \frac{\vartheta_1\alpha_C I_C^h}{1+\varphi_1 I_C^h} + \frac{\vartheta_2[\alpha_Z I_Z^h + \alpha_Z^h I_Z^v]}{1+\varphi_2 I_Z^h}\right) R \Big]\end{aligned}$$

$$
\begin{aligned}
&- \Big[\gamma_C I_C^h + \gamma_Z I_Z^h + \gamma_{CZ} I_{CZ}^h \\
&- \left(\varrho_h + \frac{\vartheta_1 \alpha_C I_C^h}{1+\varphi_1 I_C^h} + \frac{\vartheta_2[\alpha_Z I_Z^h + \alpha_Z^h I_Z^v]}{1+\varphi_2 I_Z^h} \right) R^* \Big] \Big\| \\
&\le \Big[\varrho_h + \frac{\vartheta_1 \alpha_C I_C^h}{1+\varphi_1 I_C^h} + \frac{\vartheta_2[\alpha_Z I_Z^h + \alpha_Z^h I_Z^v]}{1+\varphi_2 I_Z^h} \Big] \| R(t) - R^*(t) \| \\
&\le \big[\varrho_h + \vartheta_1 \alpha_C \| I_C^h \| + \vartheta_2 \alpha_Z \| I_Z^h \| + \vartheta_2 \alpha_Z^h \| I_Z^v \| \big] \| R(t) - R^*(t) \| \\
&\le \big[\varrho_h + \vartheta_1 \alpha_C \varkappa_2 + \vartheta_2 \alpha_Z \varkappa_3 + \vartheta_2 \alpha_Z^h \varkappa_7 \big] \| R(t) - R^*(t) \| \\
&= L_5 \| R(t) - R^*(t) \|.
\end{aligned}
$$

This shows that $\mathbf{X}_5$ is Lipschitz w.r.t. R with constant $L_5 > 0$.

For $\mathbf{X}_6$, we choose $S_v, S_v^* \in \mathbb{F} := C(J, \mathbb{R})$ arbitrarily. Then

$$
\begin{aligned}
&\| \mathbf{X}_6(t, S_v(t)) - \mathbf{X}_6(t, S_v^*(t)) \| \\
&= \left\| \left[\Psi^v - \left(\frac{\alpha_Z^v (I_Z^h + I_{CZ}^h)}{1+\varphi_2 I_Z^h + \varphi_3 I_{CZ}^h} + \varrho_v \right) S_v \right] \right. \\
&\quad \left. - \left[\Psi^v - \left(\frac{\alpha_Z^v (I_Z^h + I_{CZ}^h)}{1+\varphi_2 I_Z^h + \varphi_3 I_{CZ}^h} + \varrho_v \right) S_v^* \right] \right\| \\
&\le \Big[\frac{\alpha_Z^v (I_Z^h + I_{CZ}^h)}{1+\varphi_2 I_Z^h + \varphi_3 I_{CZ}^h} + \varrho_v \Big] \| S_v(t) - S_v^*(t) \| \\
&\le \big[\alpha_Z^v \| I_Z^h \| + \alpha_Z^v \| I_{CZ}^h \| + \varrho_v \big] \| S_v(t) - S_v^*(t) \| \\
&\le \big[\alpha_Z^v \varkappa_3 + \alpha_Z^v \varkappa_4 + \varrho_v \big] \| S_v(t) - S_v^*(t) \| \\
&= L_6 \| S_v(t) - S_v^*(t) \|.
\end{aligned}
$$

This shows that $\mathbf{X}_6$ is Lipschitz w.r.t. S_v with constant $L_6 > 0$.

Finally, for $\mathbf{X}_7$, we choose $I_Z^v, I_Z^{v*} \in \mathbb{F} := C(J, \mathbb{R})$ arbitrarily. Then

$$
\begin{aligned}
&\| \mathbf{X}_7(t, I_Z^v(t)) - \mathbf{X}_7(t, I_Z^{v*}(t)) \| \\
&= \left\| \left[\frac{\alpha_Z^v (I_Z^h + I_{CZ}^h)}{1+\varphi_2 I_Z^h + \varphi_3 I_{CZ}^h} S_v - \varrho_v I_Z^v \right] \right. \\
&\quad \left. - \left[\frac{\alpha_Z^v (I_Z^h + I_{CZ}^h)}{1+\varphi_2 I_Z^h + \varphi_3 I_{CZ}^h} S_v - \varrho_v I_Z^{v*} \right] \right\| \\
&\le \varrho_v \| I_Z^v(t) - I_Z^{v*}(t) \| \\
&= L_7 \| I_Z^v(t) - I_Z^{v*}(t) \|.
\end{aligned}
$$

This shows that $\mathbf{X}_7$ is Lipschitz w.r.t. I_Z^v with constant $L_7 > 0$. The proof for all seven functions is completed. □

Theorem 5. *Let (G3) to be held. Then the (c_1, c_2)-fractal-fractional model (13) of the co-infection Zika-COVID-19 has a unique solution when*

$$
\left[\frac{(1-c_1) c_2 \tau^{c_2-1}}{\mathbf{AB}(c_1)} + \frac{c_1 c_2 \Gamma(c_2) \tau^{c_1+c_2-1}}{\Gamma(c_1+c_2)\mathbf{AB}(c_1)} \right] L_j < 1, \quad (j \in \{1, \dots, 7\}), \tag{27}
$$

and L_j's are introduced in (26).

Proof. We assume that the conclusion of theorem is not valid. Hence there exists another solution for the (c_1, c_2)-fractal-fractional model (13) of the co-infection Zika-COVID-19. Assume that $\big(S_h^*, I_C^{h*}, I_Z^{h*}, I_{CZ}^{h*}, R^*, S_v^*, I_Z^{v*}\big)$ is another solution under the initial value condition

$$
\begin{aligned}
&\big(S_h^*(0), I_C^{h*}(0), I_Z^{h*}(0), I_{CZ}^{h*}(0), R^*(0), S_v^*(0), I_Z^{v*}(0)\big) \\
&= \big(S_{h0}, I_{C0}^h, I_{Z0}^h, I_{CZ0}^h, R_0, S_{v0}, I_{Z0}^v\big)
\end{aligned}
$$

. Then by (20), we have

$$
\begin{aligned}
S_h^*(t) &= S_{h0} + \frac{(1-c_1)c_2 t^{c_2-1}}{\mathbf{AB}(c_1)} \mathbf{X}_1(t, S_h^*(t)) \\
&\quad + \frac{c_1 c_2}{\Gamma(c_1)\mathbf{AB}(c_1)} \\
&\quad \times \int_0^t \mathfrak{q}^{c_2-1} (t-\mathfrak{q})^{c_1-1} \mathbf{X}_1(\mathfrak{q}, S_h^*(\mathfrak{q}))\, d\mathfrak{q}, \\
I_C^{h*}(t) &= I_{C0}^h + \frac{(1-c_1)c_2 t^{c_2-1}}{\mathbf{AB}(c_1)} \mathbf{X}_2(t, I_C^{h*}(t)) \\
&\quad + \frac{c_1 c_2}{\Gamma(c_1)\mathbf{AB}(c_1)} \int_0^t \mathfrak{q}^{c_2-1} (t-\mathfrak{q})^{c_1-1} \mathbf{X}_2(\mathfrak{q}, I_C^{h*}(\mathfrak{q}))\, d\mathfrak{q}, \\
I_Z^{h*}(t) &= I_{Z0}^h + \frac{(1-c_1)c_2 t^{c_2-1}}{\mathbf{AB}(c_1)} \mathbf{X}_3(t, I_Z^{h*}(t)) \\
&\quad + \frac{c_1 c_2}{\Gamma(c_1)\mathbf{AB}(c_1)} \int_0^t \mathfrak{q}^{c_2-1} (t-\mathfrak{q})^{c_1-1} \mathbf{X}_3(\mathfrak{q}, I_Z^{h*}(\mathfrak{q}))\, d\mathfrak{q}, \\
I_{CZ}^{h*}(t) &= I_{CZ0}^h + \frac{(1-c_1)c_2 t^{c_2-1}}{\mathbf{AB}(c_1)} \mathbf{X}_4(t, I_{CZ}^{h*}(t)) \\
&\quad + \frac{c_1 c_2}{\Gamma(c_1)\mathbf{AB}(c_1)} \int_0^t \mathfrak{q}^{c_2-1} (t-\mathfrak{q})^{c_1-1} \mathbf{X}_4(\mathfrak{q}, I_{CZ}^{h*}(\mathfrak{q}))\, d\mathfrak{q}, \\
R^*(t) &= R_0 + \frac{(1-c_1)c_2 t^{c_2-1}}{\mathbf{AB}(c_1)} \mathbf{X}_5(t, R^*(t)) \\
&\quad + \frac{c_1 c_2}{\Gamma(c_1)\mathbf{AB}(c_1)} \int_0^t \mathfrak{q}^{c_2-1} (t-\mathfrak{q})^{c_1-1} \mathbf{X}_5(\mathfrak{q}, R^*(\mathfrak{q}))\, d\mathfrak{q}, \\
S_v^*(t) &= S_{v0} + \frac{(1-c_1)c_2 t^{c_2-1}}{\mathbf{AB}(c_1)} \mathbf{X}_6(t, S_v^*(t)) \\
&\quad + \frac{c_1 c_2}{\Gamma(c_1)\mathbf{AB}(c_1)} \int_0^t \mathfrak{q}^{c_2-1} (t-\mathfrak{q})^{c_1-1} \mathbf{X}_6(\mathfrak{q}, S_v^*(\mathfrak{q}))\, d\mathfrak{q}, \\
I_Z^{v*}(t) &= I_{Z0}^v + \frac{(1-c_1)c_2 t^{c_2-1}}{\mathbf{AB}(c_1)} \mathbf{X}_7(t, I_Z^{v*}(t)) \\
&\quad + \frac{c_1 c_2}{\Gamma(c_1)\mathbf{AB}(c_1)} \int_0^t \mathfrak{q}^{c_2-1} (t-\mathfrak{q})^{c_1-1} \mathbf{X}_7(\mathfrak{q}, I_Z^{v*}(\mathfrak{q}))\, d\mathfrak{q}.
\end{aligned}
$$

Now, we can estimate

$$
\begin{aligned}
|S_h(t) - S_h^*(t)| &\le \frac{(1-c_1)c_2 t^{c_2-1}}{\mathbf{AB}(c_1)} \Big| \mathbf{X}_1(t, S_h(t)) - \mathbf{X}_1(t, S_h^*(t)) \Big| \\
&\quad + \frac{c_1 c_2}{\Gamma(c_1)\mathbf{AB}(c_1)} \\
&\quad \times \int_0^t \mathfrak{q}^{c_2-1} (t-\mathfrak{q})^{c_1-1} \Big| \mathbf{X}_1(\mathfrak{w}, S_h(\mathfrak{w})) - \mathbf{X}_1(\mathfrak{w}, S_h^*(\mathfrak{w})) \Big|\, d\mathfrak{w} \\
&\le \frac{(1-c_1)c_2 t^{c_2-1}}{\mathbf{AB}(c_1)} L_1 \| S_h - S_h^* \| \\
&\quad + \frac{c_1 c_2}{\Gamma(c_1)\mathbf{AB}(c_1)} \int_0^t \mathfrak{q}^{c_2-1} (t-\mathfrak{q})^{c_1-1} L_1 \| S_h - S_h^* \|\, d\mathfrak{w} \\
&\le \left[\frac{(1-c_1)c_2 \tau^{c_2-1}}{\mathbf{AB}(c_1)} + \frac{c_1 c_2 \Gamma(c_2) \tau^{c_1+c_2-1}}{\Gamma(c_1+c_2)\mathbf{AB}(c_1)} \right] L_1 \| S_h - S_h^* \|,
\end{aligned}
$$

and so

$$
\left(1 - \left[\frac{(1-c_1)c_2 \tau^{c_2-1}}{\mathbf{AB}(c_1)} + \frac{c_1 c_2 \Gamma(c_2) \tau^{c_1+c_2-1}}{\Gamma(c_1+c_2)\mathbf{AB}(c_1)} \right] L_1 \right) \| S_h - S_h^* \| \le 0.
$$

The above inequality holds when $\| S_h - S_h^* \| = 0$, or $S_h = S_h^*$. In the similar manner, from the inequality

$$
\| I_C^h - I_C^{h*} \| \le \left[\frac{(1-c_1)c_2 \tau^{c_2-1}}{\mathbf{AB}(c_1)} + \frac{c_1 c_2 \Gamma(c_2) \tau^{c_1+c_2-1}}{\Gamma(c_1+c_2)\mathbf{AB}(c_1)} \right] L_2 \| I_C^h - I_C^{h*} \|,
$$

we reach to

$$
\left(1 - \left[\frac{(1-c_1)c_2 \tau^{c_2-1}}{\mathbf{AB}(c_1)} + \frac{c_1 c_2 \Gamma(c_2) \tau^{c_1+c_2-1}}{\Gamma(c_1+c_2)\mathbf{AB}(c_1)} \right] L_2 \right) \| I_C^h - I_C^{h*} \| \le 0.
$$

This is true when $\| I_C^h - I_C^{h*} \| = 0$ or $I_C^h = I_C^{h*}$. Moreover, the inequality

$$
\| I_Z^h - I_Z^{h*} \| \le \left[\frac{(1-c_1)c_2 \tau^{c_2-1}}{\mathbf{AB}(c_1)} + \frac{c_1 c_2 \Gamma(c_2) \tau^{c_1+c_2-1}}{\Gamma(c_1+c_2)\mathbf{AB}(c_1)} \right] L_3 \| I_Z^h - I_Z^{h*} \|,
$$

yields

$$
\left(1 - \left[\frac{(1-c_1)c_2 \tau^{c_2-1}}{\mathbf{AB}(c_1)} + \frac{c_1 c_2 \Gamma(c_2) \tau^{c_1+c_2-1}}{\Gamma(c_1+c_2)\mathbf{AB}(c_1)} \right] L_3 \right) \| I_Z^h - I_Z^{h*} \| \le 0.
$$

Hence $I_Z^h = I_Z^{h*}$. Accordingly, we get $I_{CZ}^h = I_{CZ}^{h*}$, $R = R^*$, $S_v = S_v^*$ and $I_Z^v - I_Z^{v*}$. Consequently, for each $t \in J$, we get

$$
\begin{aligned}
&\big(S_h(t), I_C^h(t), I_Z^h(t), I_{CZ}^h(t), R(t), S_v(t), I_Z^v(t)\big) \\
&= \big(S_h^*(t), I_C^{h*}(t), I_Z^{h*}(t), I_{CZ}^{h*}(t), R^*(t), S_v^*(t), I_Z^{v*}(t)\big).
\end{aligned}
$$

This means that the (c_1, c_2)-fractal-fractional model (13) of the co-infection Zika-COVID-19 has a unique solution if (27) holds. □

UH-stable solutions

In the sequel, we investigate the UH-stability notion in relation to the system of the (c_1, c_2)-fractal-fractional model (13) of the co-infection Zika-COVID-19.

Definition 5. The (c_1, c_2)-fractal-fractional model (13) of the co-infection Zika-COVID-19 is UH-stable if $\exists\, 0 < Q_{\mathbf{X}_j} \in \mathbb{R}, j \in \{1, \dots, 7\}$ s.t. $\forall\, R_j > 0$, and $\forall \left(S_h^*, I_C^{h*}, I_Z^{h*}, I_{CZ}^{h*}, R^*, S_v^*, I_Z^{v*}\right) \in \mathcal{X}$ satisfying

$$\begin{cases}
\left|{}^{\mathbf{FFML}}D_{0,t}^{(c_1,c_2)} S_h^*(t) - \mathbf{X}_1\left(t, S_h^*(t)\right)\right| < R_1,\\
\left|{}^{\mathbf{FFML}}D_{0,t}^{(c_1,c_2)} I_C^{h*}(t) - \mathbf{X}_2\left(t, I_C^{h*}(t)\right)\right| < R_2,\\
\left|{}^{\mathbf{FFML}}D_{0,t}^{(c_1,c_2)} I_Z^{h*}(t) - \mathbf{X}_3\left(t, I_Z^{h*}(t)\right)\right| < R_3,\\
\left|{}^{\mathbf{FFML}}D_{0,t}^{(c_1,c_2)} I_{CZ}^{h*}(t) - \mathbf{X}_4\left(t, I_{CZ}^{h*}(t)\right)\right| < R_4,\\
\left|{}^{\mathbf{FFML}}D_{0,t}^{(c_1,c_2)} R^*(t) - \mathbf{X}_5\left(t, R^*(t)\right)\right| < R_5,\\
\left|{}^{\mathbf{FFML}}D_{0,t}^{(c_1,c_2)} S_v^*(t) - \mathbf{X}_6\left(t, S_v^*(t)\right)\right| < R_6,\\
\left|{}^{\mathbf{FFML}}D_{0,t}^{(c_1,c_2)} I_Z^{v*}(t) - \mathbf{X}_7\left(t, I_Z^{v*}(t)\right)\right| < R_7,
\end{cases} \tag{28}$$

$\exists \left(S_h, I_C^h, I_Z^h, I_{CZ}^h, R, S_v, I_Z^v\right) \in \mathcal{X}$ satisfying the (c_1, c_2)-fractal-fractional model (13) of the co-infection Zika-COVID-19 with

$$\begin{cases}
\left|S_h^* - S_h\right| \le Q_{\mathbf{X}_1} R_1, \qquad \left|I_C^{h*} - I_C^h\right| \le Q_{\mathbf{X}_2} R_2,\\
\left|I_Z^{h*} - I_Z^h\right| \le Q_{\mathbf{X}_3} R_3, \qquad \left|I_{CZ}^{h*} - I_{CZ}^h\right| \le Q_{\mathbf{X}_4} R_4,\\
\left|R^* - R\right| \le Q_{\mathbf{X}_5} R_5, \qquad \left|S_v^* - S_v\right| \le Q_{\mathbf{X}_6} R_6,\\
\left|I_Z^{v*} - I_Z^v\right| \le Q_{\mathbf{X}_7} R_7.
\end{cases}$$

Remark 1. $\left(S_h^*, I_C^{h*}, I_Z^{h*}, I_{CZ}^{h*}, R^*, S_v^*, I_Z^{v*}\right) \in \mathcal{X}$ is termed as a solution for (28) iff $\exists\, \mathcal{G}_1, \dots \mathcal{G}_7 \in C([0,\tau], \mathbb{R})$ (depending on $S_h^*, I_C^{h*}, I_Z^{h*}, I_{CZ}^{h*}, R^*, S_v^*, I_Z^{v*}$, respectively) so that $\forall\, t \in J$,

(i) $|\mathcal{G}_j(t)| < R_j$,

(ii) We have

$$\begin{cases}
{}^{\mathbf{FFML}}D_{0,t}^{(c_1,c_2)} S_h^*(t) = \mathbf{X}_1\left(t, S_h^*(t)\right) + \mathcal{G}_1(t),\\
{}^{\mathbf{FFML}}D_{0,t}^{(c_1,c_2)} I_C^{h*}(t) = \mathbf{X}_2\left(t, I_C^{h*}(t)\right) + \mathcal{G}_2(t),\\
{}^{\mathbf{FFML}}D_{0,t}^{(c_1,c_2)} I_Z^{h*}(t) = \mathbf{X}_3\left(t, I_Z^{h*}(t)\right) + \mathcal{G}_3(t),\\
{}^{\mathbf{FFML}}D_{0,t}^{(c_1,c_2)} I_{CZ}^{h*}(t) = \mathbf{X}_4\left(t, I_{CZ}^{h*}(t)\right) + \mathcal{G}_4(t),\\
{}^{\mathbf{FFML}}D_{0,t}^{(c_1,c_2)} R^*(t) = \mathbf{X}_5\left(t, R^*(t)\right) + \mathcal{G}_5(t),\\
{}^{\mathbf{FFML}}D_{0,t}^{(c_1,c_2)} S_v^*(t) = \mathbf{X}_6\left(t, S_v^*(t)\right) + \mathcal{G}_6(t),\\
{}^{\mathbf{FFML}}D_{0,t}^{(c_1,c_2)} I_Z^{v*}(t) = \mathbf{X}_7\left(t, I_Z^{v*}(t)\right) + \mathcal{G}_7(t).
\end{cases}$$

The following lemma is useful for our main theorem.

Lemma 2. *For each $R_1, \dots, R_7 > 0$, suppose that $\left(S_h^*, I_C^{h*}, I_Z^{h*}, I_{CZ}^{h*}, R^*, S_v^*, I_Z^{v*}\right) \in \mathcal{X}$ is considered as a solution of (28). Then the functions $S_h^*, I_C^{h*}, I_Z^{h*}, I_{CZ}^{h*}, R^*, S_v^*, I_Z^{v*} \in \mathbb{F}$ fulfill the inequalities*

$$\begin{aligned}
&\Bigg|S_h^*(t) - \Bigg(S_{h0} + \frac{(1-c_1)c_2 t^{c_2-1}}{\mathbf{AB}(c_1)}\mathbf{X}_1(t, S_h^*(t))\\
&\quad + \frac{c_1 c_2}{\Gamma(c_1)\mathbf{AB}(c_1)}\int_0^t \mathfrak{q}^{c_2-1}(t-\mathfrak{q})^{c_1-1}\mathbf{X}_1(\mathfrak{q}, S_h^*(\mathfrak{q}))\,d\mathfrak{q}\Bigg)\Bigg|\\
&\quad \le \left[\frac{(1-c_1)c_2\tau^{c_2-1}}{\mathbf{AB}(c_1)} + \frac{c_1 c_2 \Gamma(c_2)\tau^{c_1+c_2-1}}{\Gamma(c_1+c_2)\mathbf{AB}(c_1)}\right]R_1,
\end{aligned} \tag{29}$$

and

$$\begin{aligned}
&\Bigg|I_C^{h*}(t) - \Bigg(I_{C0}^h + \frac{(1-c_1)c_2 t^{c_2-1}}{\mathbf{AB}(c_1)}\mathbf{X}_2(t, I_C^{h*}(t))\\
&\quad + \frac{c_1 c_2}{\Gamma(c_1)\mathbf{AB}(c_1)}\int_0^t \mathfrak{q}^{c_2-1}(t-\mathfrak{q})^{c_1-1}\mathbf{X}_2(\mathfrak{q}, I_C^{h*}(\mathfrak{q}))\,d\mathfrak{q}\Bigg)\Bigg|\\
&\quad \le \left[\frac{(1-c_1)c_2\tau^{c_2-1}}{\mathbf{AB}(c_1)} + \frac{c_1 c_2 \Gamma(c_2)\tau^{c_1+c_2-1}}{\Gamma(c_1+c_2)\mathbf{AB}(c_1)}\right]R_2,
\end{aligned} \tag{30}$$

and

$$\begin{aligned}
&\Bigg|I_Z^{h*}(t) - \Bigg(I_{Z0}^h + \frac{(1-c_1)c_2 t^{c_2-1}}{\mathbf{AB}(c_1)}\mathbf{X}_3(t, I_Z^{h*}(t))\\
&\quad + \frac{c_1 c_2}{\Gamma(c_1)\mathbf{AB}(c_1)}\int_0^t \mathfrak{q}^{c_2-1}(t-\mathfrak{q})^{c_1-1}\mathbf{X}_3(\mathfrak{q}, I_Z^{h*}(\mathfrak{q}))\,d\mathfrak{q}\Bigg)\Bigg|\\
&\quad \le \left[\frac{(1-c_1)c_2\tau^{c_2-1}}{\mathbf{AB}(c_1)} + \frac{c_1 c_2 \Gamma(c_2)\tau^{c_1+c_2-1}}{\Gamma(c_1+c_2)\mathbf{AB}(c_1)}\right]R_3,
\end{aligned} \tag{31}$$

and

$$\begin{aligned}
&\Bigg|I_{CZ}^{h*}(t) - \Bigg(I_{CZ0}^h + \frac{(1-c_1)c_2 t^{c_2-1}}{\mathbf{AB}(c_1)}\mathbf{X}_4(t, I_{CZ}^{h*}(t))\\
&\quad + \frac{c_1 c_2}{\Gamma(c_1)\mathbf{AB}(c_1)}\int_0^t \mathfrak{q}^{c_2-1}(t-\mathfrak{q})^{c_1-1}\mathbf{X}_4(\mathfrak{q}, I_{CZ}^{h*}(\mathfrak{q}))\,d\mathfrak{q}\Bigg)\Bigg|\\
&\quad \le \left[\frac{(1-c_1)c_2\tau^{c_2-1}}{\mathbf{AB}(c_1)} + \frac{c_1 c_2 \Gamma(c_2)\tau^{c_1+c_2-1}}{\Gamma(c_1+c_2)\mathbf{AB}(c_1)}\right]R_4,
\end{aligned} \tag{32}$$

and

$$\begin{aligned}
&\Bigg|R^*(t) - \Bigg(R_0 + \frac{(1-c_1)c_2 t^{c_2-1}}{\mathbf{AB}(c_1)}\mathbf{X}_5(t, R^*(t))\\
&\quad + \frac{c_1 c_2}{\Gamma(c_1)\mathbf{AB}(c_1)}\int_0^t \mathfrak{q}^{c_2-1}(t-\mathfrak{q})^{c_1-1}\mathbf{X}_5(\mathfrak{q}, R^*(\mathfrak{q}))\,d\mathfrak{q}\Bigg)\Bigg|\\
&\quad \le \left[\frac{(1-c_1)c_2\tau^{c_2-1}}{\mathbf{AB}(c_1)} + \frac{c_1 c_2 \Gamma(c_2)\tau^{c_1+c_2-1}}{\Gamma(c_1+c_2)\mathbf{AB}(c_1)}\right]R_5,
\end{aligned} \tag{33}$$

and

$$\begin{aligned}
&\Bigg|S_v^*(t) - \Bigg(S_{v0} + \frac{(1-c_1)c_2 t^{c_2-1}}{\mathbf{AB}(c_1)}\mathbf{X}_6(t, S_v^*(t))\\
&\quad + \frac{c_1 c_2}{\Gamma(c_1)\mathbf{AB}(c_1)}\int_0^t \mathfrak{q}^{c_2-1}(t-\mathfrak{q})^{c_1-1}\mathbf{X}_6(\mathfrak{q}, S_v^*(\mathfrak{q}))\,d\mathfrak{q}\Bigg)\Bigg|\\
&\quad \le \left[\frac{(1-c_1)c_2\tau^{c_2-1}}{\mathbf{AB}(c_1)} + \frac{c_1 c_2 \Gamma(c_2)\tau^{c_1+c_2-1}}{\Gamma(c_1+c_2)\mathbf{AB}(c_1)}\right]R_6,
\end{aligned} \tag{34}$$

and

$$\begin{aligned}
&\Bigg|I_Z^{v*}(t) - \Bigg(I_{Z0}^v + \frac{(1-c_1)c_2 t^{c_2-1}}{\mathbf{AB}(c_1)}\mathbf{X}_7(t, I_Z^{v*}(t))\\
&\quad + \frac{c_1 c_2}{\Gamma(c_1)\mathbf{AB}(c_1)}\int_0^t \mathfrak{q}^{c_2-1}(t-\mathfrak{q})^{c_1-1}\mathbf{X}_7(\mathfrak{q}, I_Z^{v*}(\mathfrak{q}))\,d\mathfrak{q}\Bigg)\Bigg|\\
&\quad \le \left[\frac{(1-c_1)c_2\tau^{c_2-1}}{\mathbf{AB}(c_1)} + \frac{c_1 c_2 \Gamma(c_2)\tau^{c_1+c_2-1}}{\Gamma(c_1+c_2)\mathbf{AB}(c_1)}\right]R_7.
\end{aligned} \tag{35}$$

Proof. Let $R_1 > 0$ be arbitrary. Since $S_h^* \in \mathbb{F}$ satisfies

$$\left|{}^{\mathbf{FFML}}D_{0,t}^{(c_1,c_2)} S_h^*(t) - \mathbf{X}_1\left(t, S_h^*(t)\right)\right| < R_1,$$

so, by Remark 1, we are allowed to select a function $\mathcal{G}_1(t)$ so that

$${}^{\mathbf{FFML}}D_{0,t}^{(c_1,c_2)} S_h^*(t) = \mathbf{X}_1\left(t, S_h^*(t)\right) + \mathcal{G}_1(t),$$

and $|\mathcal{G}_1(t)| \le R_1$. It follows that

$$\begin{aligned}
S_h^*(t) &= S_{h0} + \frac{(1-c_1)c_2 t^{c_2-1}}{\mathbf{AB}(c_1)}\left[\mathbf{X}_1(t, S_h^*(t)) + \mathcal{G}_1(t)\right]\\
&\quad + \frac{c_1 c_2}{\Gamma(c_1)\mathbf{AB}(c_1)}\int_0^t \mathfrak{q}^{c_2-1}(t-\mathfrak{q})^{c_1-1}\left[\mathbf{X}_1(\mathfrak{q}, S_h^*(\mathfrak{q})) + \mathcal{G}_1(\mathfrak{q})\right]d\mathfrak{q}.
\end{aligned}$$

Then, we estimate

$$\begin{aligned}
&\Bigg|S_h^*(t) - \Bigg(S_{h0} + \frac{(1-c_1)c_2 t^{c_2-1}}{\mathbf{AB}(c_1)}\mathbf{X}_1(t, S_h^*(t))\\
&\quad + \frac{c_1 c_2}{\Gamma(c_1)\mathbf{AB}(c_1)}\int_0^t \mathfrak{q}^{c_2-1}(t-\mathfrak{q})^{c_1-1}\mathbf{X}_1(\mathfrak{q}, S_h^*(\mathfrak{q}))\,d\mathfrak{q}\Bigg)\Bigg|
\end{aligned}$$

$$\leq \frac{(1-c_1)c_2t^{c_2-1}}{\mathbf{AB}(c_1)}|\mathcal{G}_1(t)| + \frac{c_1c_2}{\Gamma(c_1)\mathbf{AB}(c_1)}\int_0^t \mathfrak{q}^{c_2-1}(t-\mathfrak{q})^{c_1-1}|\mathcal{G}_1(\mathfrak{q})|\,d\mathfrak{q}$$
$$\leq \frac{(1-c_1)c_2\tau^{c_2-1}}{\mathbf{AB}(c_1)}R_1 + \frac{c_1c_2\tau^{c_1+c_2-1}\Gamma(c_2)}{\Gamma(c_1+c_2)\mathbf{AB}(c_1)}R_1$$
$$= \Big[\frac{(1-c_1)c_2\tau^{c_2-1}}{\mathbf{AB}(c_1)} + \frac{c_1c_2\Gamma(c_2)\tau^{c_1+c_2-1}}{\Gamma(c_1+c_2)\mathbf{AB}(c_1)}\Big]R_1.$$

This means that the inequality (29) is achieved. Similarly, we can obtain the inequalities (30)–(35). □

The UH-stability is checked about the (c_1, c_2)-fractal-fractional model (13) of the co-infection Zika-COVID-19.

Theorem 6. *Let (G3) be fulfilled. Then the (c_1, c_2)-fractal-fractional model (13) of the co-infection Zika-COVID-19 is UH-stable on $J := [0, \tau]$ such that*

$$\Big[\frac{(1-c_1)c_2\tau^{c_2-1}}{\mathbf{AB}(c_1)} + \frac{c_1c_2\Gamma(c_2)\tau^{c_1+c_2-1}}{\Gamma(c_1+c_2)\mathbf{AB}(c_1)}\Big]L_j < 1, \quad j \in \{1, \dots, 7\},$$

in which L_j's are introduced by (26).

Proof. Let $R_1 > 0$ and $S_h^* \in \mathbb{F}$ be an arbitrary solution of (28). Also, from Theorem 5, we assume $S_h \in \mathbb{F}$ as a unique solution of the (c_1, c_2)-fractal-fractional model (13) of the co-infection Zika-COVID-19. Then $S_h(t)$ is defined as

$$S_h(t) = \varkappa_1 + \frac{(1-c_1)c_2t^{c_2-1}}{\mathbf{AB}(c_1)}\mathbf{X}_1(t, S_h(t)) + \frac{c_1c_2}{\Gamma(c_1)\mathbf{AB}(c_1)}\int_0^t \mathfrak{q}^{c_2-1}(t-\mathfrak{q})^{c_1-1}\mathbf{X}_1(\mathfrak{q}, S_h(\mathfrak{q}))\,d\mathfrak{q}.$$

Therefore, by Lemma 2 and with the help of the triangle inequality, we estimate

$$\begin{aligned}
\big|S_h^*(t) - S_h(t)\big| &\leq \Big|S_h^*(t) - S_{h0} - \frac{(1-c_1)c_2t^{c_2-1}}{\mathbf{AB}(c_1)}\mathbf{X}_1(t, S_h(t)) \\
&\quad - \frac{c_1c_2}{\Gamma(c_1)\mathbf{AB}(c_1)}\int_0^t \mathfrak{q}^{c_2-1}(t-\mathfrak{q})^{c_1-1}\mathbf{X}_1(\mathfrak{q}, S_h(\mathfrak{q}))\,d\mathfrak{q}\Big| \\
&\leq \Big|S_h^*(t) - \Big(S_{h0} + \frac{(1-c_1)c_2t^{c_2-1}}{\mathbf{AB}(c_1)}\mathbf{X}_1(t, S_h^*(t)) \\
&\quad + \frac{c_1c_2}{\Gamma(c_1)\mathbf{AB}(c_1)}\int_0^t \mathfrak{q}^{c_2-1}(t-\mathfrak{q})^{c_1-1}\mathbf{X}_1(\mathfrak{q}, S_h^*(\mathfrak{q}))\,d\mathfrak{q}\Big)\Big| \\
&\quad + \frac{(1-c_1)c_2t^{c_2-1}}{\mathbf{AB}(c_1)}\big|\mathbf{X}_1(t, S_h^*(t)) - \mathbf{X}_1(t, S_h(t))\big| \\
&\quad + \frac{c_1c_2}{\Gamma(c_1)\mathbf{AB}(c_1)}\int_0^t \mathfrak{q}^{c_2-1}(t-\mathfrak{q})^{c_1-1}\big|\mathbf{X}_1(\mathfrak{q}, S_h^*(\mathfrak{q})) \\
&\quad - \mathbf{X}_1(\mathfrak{q}, S_h(\mathfrak{q}))\big|\,d\mathfrak{w} \\
&\leq \Big[\frac{(1-c_1)c_2\tau^{c_2-1}}{\mathbf{AB}(c_1)} + \frac{c_1c_2\Gamma(c_2)\tau^{c_1+c_2-1}}{\Gamma(c_1+c_2)\mathbf{AB}(c_1)}\Big]R_1 \\
&\quad + \frac{(1-c_1)c_2\tau^{c_2-1}}{\mathbf{AB}(c_1)}L_1\|S_h^* - S_h\| \\
&\quad + \frac{c_1c_2\tau^{c_1+c_2-1}\Gamma(c_2)}{\Gamma(c_1+c_2)\mathbf{AB}(c_1)}L_1\|S_h^* - S_h\| \\
&\leq \Big[\frac{(1-c_1)c_2\tau^{c_2-1}}{\mathbf{AB}(c_1)} + \frac{c_1c_2\Gamma(c_2)\tau^{c_1+c_2-1}}{\Gamma(c_1+c_2)\mathbf{AB}(c_1)}\Big]R_1 \\
&\quad + \Big[\frac{(1-c_1)c_2\tau^{c_2-1}}{\mathbf{AB}(c_1)} + \frac{c_1c_2\Gamma(c_2)\tau^{c_1+c_2-1}}{\Gamma(c_1+c_2)\mathbf{AB}(c_1)}\Big]L_1\|S_h^* - S_h\|.
\end{aligned}$$

Hence, we get

$$\|S_h^* - S_h\| \leq \frac{\Big[\frac{(1-c_1)c_2\tau^{c_2-1}}{\mathbf{AB}(c_1)} + \frac{c_1c_2\Gamma(c_2)\tau^{c_1+c_2-1}}{\Gamma(c_1+c_2)\mathbf{AB}(c_1)}\Big]R_1}{1 - \Big[\frac{(1-c_1)c_2\tau^{c_2-1}}{\mathbf{AB}(c_1)} + \frac{c_1c_2\Gamma(c_2)\tau^{c_1+c_2-1}}{\Gamma(c_1+c_2)\mathbf{AB}(c_1)}\Big]L_1}.$$

If we let $Q_{\mathbf{X}_1} = \dfrac{\Big[\frac{(1-c_1)c_2\tau^{c_2-1}}{\mathbf{AB}(c_1)} + \frac{c_1c_2\Gamma(c_2)\tau^{c_1+c_2-1}}{\Gamma(c_1+c_2)\mathbf{AB}(c_1)}\Big]}{1 - \Big[\frac{(1-c_1)c_2\tau^{c_2-1}}{\mathbf{AB}(c_1)} + \frac{c_1c_2\Gamma(c_2)\tau^{c_1+c_2-1}}{\Gamma(c_1+c_2)\mathbf{AB}(c_1)}\Big]L_1}$, then $\|S_h^* - S_h\| \leq Q_{\mathbf{X}_1}R_1$. Similarly, we have

$$\|I_C^{h*} - I_C^h\| \leq Q_{\mathbf{X}_2}R_2,$$

$$\|I_Z^{h*} - I_Z^h\| \leq Q_{\mathbf{X}_3}R_3,$$

$$\|I_{CZ}^{h*} - I_{CZ}^h\| \leq Q_{\mathbf{X}_4}R_4,$$

$$\|R^* - R\| \leq Q_{\mathbf{X}_5}R_5,$$

$$\|S_v^* - S_v\| \leq Q_{\mathbf{X}_6}R_6,$$

$$\|I_Z^{v*} - I_Z^v\| \leq Q_{\mathbf{X}_7}R_7,$$

where

$$Q_{\mathbf{X}_j} = \frac{\Big[\frac{(1-c_1)c_2\tau^{c_2-1}}{\mathbf{AB}(c_1)} + \frac{c_1c_2\Gamma(c_2)\tau^{c_1+c_2-1}}{\Gamma(c_1+c_2)\mathbf{AB}(c_1)}\Big]}{1 - \Big[\frac{(1-c_1)c_2\tau^{c_2-1}}{\mathbf{AB}(c_1)} + \frac{c_1c_2\Gamma(c_2)\tau^{c_1+c_2-1}}{\Gamma(c_1+c_2)\mathbf{AB}(c_1)}\Big]L_j}, \quad (j \in \{2, \dots, 7\}).$$

Hence, the UH-stability of the (c_1, c_2)-fractal-fractional model (13) of the co-infection Zika-COVID-19 is fulfilled. □

Numerical scheme via Newton polynomials method

This section shows the numerical procedures of the proposed fractal-fractional co-infection model for COVID-19 and Zika virus dynamics. Thus, the initial value problem of the fractal-fractional derivative is written as

$$\begin{cases} {}^{\mathbf{FFML}}_{0}D_{\varpi}^{(c_1,c_2)}\Theta^*(\varpi) = \Delta^*(\varpi, \Theta^*(\varpi)), \\ \Theta^*(0) = \Theta_0^*. \end{cases} \tag{36}$$

Here, the variable ϖ denotes the time t.

Now, fractal-fractional integral of the initial value problem (36) gives that

$$\Theta^*(\varpi) - \Theta^*(0) = \frac{(1-c_1)}{\mathbf{AB}(c_1)}c_2\varpi^{c_2-1}\Delta^*(\varpi, \Theta^*(\varpi)) + \frac{c_1c_2}{\Gamma(c_1)\mathbf{AB}(c_1)}\int_0^{\varpi} \varpi^{*c_2-1}(\varpi - \varpi^*)^{c_1-1}\Delta^*(\varpi^*, \Theta^*(\varpi^*))d\varpi^*. \tag{37}$$

Eq. (37) at the point $\varpi_{p+1} = (p+1)h$, and taking $\delta^*(\varpi, \Theta^*(\varpi)) = c_2\varpi^{c_2-1}\Delta^*(\varpi, \Theta^*(\varpi))$ results in

$$\Theta^*(\varpi_{n+1}) - \Theta^*(0) = \frac{(1-c_1)}{\mathbf{AB}(c_1)}\delta^*(\varpi, \Theta^*(\varpi)) + \frac{c_1}{\Gamma(c_1)\mathbf{AB}(c_1)}\int_0^{\varpi_{n+1}} \delta^*(\varpi^*, \Theta^*(\varpi^*))(\varpi_{p+1} - \varpi^*)^{c_1-1}d\varpi^*. \tag{38}$$

Eq. (38) can now be expressed as

$$\Theta^*(\varpi_{p+1}) = \Theta^*(0) + \frac{(1-c_1)}{\mathbf{AB}(c_1)}\delta^*(\varpi_p, \Theta^{*p}) + \frac{c_1}{\mathbf{AB}(c_1)\Gamma(c_1)}\sum_{q=2}^{p}\int_{\varpi_q}^{\varpi_{q+1}} \delta^*(\varpi^*, \Theta^*(\varpi^*))(\varpi_{p+1} - \varpi^*)^{c_1-1}d\varpi^*. \tag{39}$$

Now, making use of the Newton polynomial, Eq. (39) is rewritten as:

$$\Theta^{*p+1} = \Theta_0^* + \frac{(1-c_1)}{\mathbf{AB}(c_1)}\delta^*(\varpi_p, \Theta^{*p}) + \frac{c_1}{\mathbf{AB}(c_1)\Gamma(c_1)}$$

$$\sum_{q=2}^{p}\begin{Bmatrix}\int_{\varpi_q}^{\varpi_{q+1}}\delta^*(\varpi_{q-2},\Theta^{*q-2})(\varpi_{p+1}-\mathfrak{W}^*)^{c_1-1}d\mathfrak{W}^*\\ +\int_{\varpi_q}^{\varpi_{q+1}}\frac{\delta^*(\varpi_{q-1},\Theta^{*q-1})-\delta^*(\varpi_{q-2},\Theta^{*q-2})}{h}\\ \times(\mathfrak{W}^*-\varpi_{q-2})(\varpi_{p+1}-\mathfrak{W}^*)^{c_1-1}d\mathfrak{W}^*\\ +\int_{\varpi_q}^{\varpi_{q+1}}\frac{\delta^*(\varpi_q,\Theta^{*q})-2\delta^*(\varpi_{q-1},\Theta^{*q-1})+\delta^*(\varpi_{q-2},\Theta^{*q-2})}{2h^2}\\ \times(\mathfrak{W}^*-\varpi_{q-2})(\mathfrak{W}^*-\varpi_{q-1})(\varpi_{p+1}-\mathfrak{W}^*)^{c_1-1}d\mathfrak{W}^*\end{Bmatrix}. \tag{40}$$

Equivalently Eq. (40) can be written in simple terms as:

$$\begin{aligned}\Theta^{*p+1}=&\Theta_0^*+\frac{(1-c_1)}{\mathbf{AB}(c_1)}\delta^*(\varpi_p,\Theta^{*p})+\frac{c_1}{\mathbf{AB}(c_1)\Gamma(c_1)}\sum_{q=2}^{p}\delta^*\left(\varpi_{q-2},\Theta^{*q-2}\right)\\&\times\int_{\varpi_q}^{\varpi_{q+1}}(\varpi_{p+1}-\mathfrak{W}^*)^{c_1-1}d\mathfrak{W}^*\\&+\frac{c_1}{\mathbf{AB}(c_1)\Gamma(c_1)}\sum_{q=2}^{p}\frac{\delta^*\left(\varpi_{q-1},\Theta^{*q-1}\right)-\delta^*\left(\varpi_{q-2},\Theta^{*q-2}\right)}{h}\\&\times\int_{\varpi_q}^{\varpi_{q+1}}\left(\mathfrak{W}^*-\varpi_{q-2}\right)\left(\varpi_{p+1}-\mathfrak{W}^*\right)^{c_1-1}d\mathfrak{W}^*\\&+\frac{c_1}{\mathbf{AB}(c_1)\Gamma(c_1)}\sum_{q=2}^{p}\frac{\delta^*\left(\varpi_q,\Theta^{*q}\right)-2\delta^*\left(\varpi_{q-1},\Theta^{*q-1}\right)+\delta^*\left(\varpi_{q-2},\Theta^{*q-2}\right)}{2h^2}\\&\times\int_{\varpi_q}^{\varpi_{q+1}}\left(\mathfrak{W}^*-\varpi_{q-2}\right)\left(\mathfrak{W}^*-\varpi_{q-1}\right)\left(\varpi_{p+1}-\mathfrak{W}^*\right)^{c_1-1}d\mathfrak{W}^*.\end{aligned} \tag{41}$$

Now decomposing the integral in Eq. (41), leads to the following approximations:

$$\begin{aligned}\Theta^{*p+1}=&\Theta_0^*+\frac{(1-c_1)}{\mathbf{AB}(c_1)}\delta^*(\varpi_p,\Theta^{*p})\\&+\frac{c_1h^{c_1}}{\mathbf{AB}(c_1)\Gamma(c_1+1)}\sum_{q=2}^{p}\delta^*\left(\varpi_{q-2},\Theta^{*q-2}\right)\\&\times\left[(p-q+1)^{c_1}-(p-q)^{c_1}\right]\\&+\frac{c_1h^{c_1}}{\mathbf{AB}(c_1)\Gamma(c_1+2)}\sum_{q=2}^{p}\left[\delta^*\left(\varpi_{q-1},\Theta^{*q-1}\right)-\delta^*\left(\varpi_{q-2},\Theta^{*q-2}\right)\right]\\&\times\begin{bmatrix}\left(p-q+1\right)^{c_1}\left(p-q+3+2c_1\right)\\-\left(p-q\right)^{c_1}\left(p-q+3+3c_1\right)\end{bmatrix}\\&+\frac{c_1h^{c_1}}{2\mathbf{AB}(c_1)\Gamma(c_1+3)}\sum_{q=2}^{p}\Big[\delta^*\left(\varpi_q,\Theta^{*q}\right)\\&-2\delta^*\left(\varpi_{q-1},\Theta^{*q-1}\right)+\delta^*\left(\varpi_{q-2},\Theta^{*q-2}\right)\Big]\\&\times\begin{bmatrix}\left(p-q+1\right)^{c_1}\left[2(p-q)^2+(3c_1-10)(p-q)+2c_1^2+9c_1+12\right]\\-\left(p-q\right)^{c_1}\left[2(p-q)^2+(5c_1-10)(p-q)+6c_1^2+18c_1+12\right]\end{bmatrix}.\end{aligned} \tag{42}$$

Lastly, substituting $\delta^*(\varpi,\Theta^*(\varpi))=c_2\varpi^{c_2-1}\Delta^*(\varpi,\Theta^*(\varpi))$ in (42) gives the general Newton polynomial numerical scheme for the co-infection fractal-fractional model:

$$\begin{aligned}\Theta^{*p+1}=&\Theta_0^*+\frac{(1-c_1)}{\mathbf{AB}(c_1)}c_2\varpi_p^{c_2-1}\Delta^*(\varpi_p,\Theta^*(\varpi))\\&+\frac{c_1h^{c_1}}{\mathbf{AB}(c_1)\Gamma(c_1+1)}\sum_{q=2}^{p}c_2\varpi_{q-2}^{c_2-1}\Delta^*\left(\varpi_{q-2},\Theta^{*q-2}\right)\\&\times\left[(p-q+1)^{c_1}-(p-q)^{c_1}\right]\\&+\frac{c_1h^{c_1}}{\mathbf{AB}(c_1)\Gamma(c_1+2)}\sum_{q=2}^{p}\Big[c_2\varpi_{q-1}^{c_2-1}\Delta^*\left(\varpi_{q-1},\Theta^{*q-1}\right)\\&-c_2\varpi_{q-2}^{c_2-1}\Delta^*\left(\varpi_{q-2},\Theta^{*q-2}\right)\Big]\\&\times\begin{bmatrix}\left(p-q+1\right)^{c_1}\left(p-q+3+2c_1\right)\\-\left(p-q\right)^{c_1}\left(p-q+3+3c_1\right)\end{bmatrix}\\&+\frac{c_1h^{c_1}}{2\mathbf{AB}(c_1)\Gamma(c_1+3)}\\&\sum_{q=2}^{p}\Big[c_2\varpi_q^{c_2-1}\Delta^*\left(\varpi_q,\Theta^{*q}\right)-2c_2\varpi_{q-1}^{c_2-1}\Delta^*\left(\varpi_{q-1},\Theta^{*q-1}\right)\\&+c_2\varpi_{q-2}^{c_2-1}\Delta^*\left(\varpi_{q-2},\Theta^{*q-2}\right)\Big]\\&\times\begin{bmatrix}\left(p-q+1\right)^{c_1}\left[2(p-q)^2+(3c_1-10)(p-q)+2c_1^2+9c_1+12\right]\\-\left(p-q\right)^{c_1}\left[2(p-q)^2+(5c_1-10)(p-q)+6c_1^2+18c_1+12\right]\end{bmatrix}.\end{aligned} \tag{43}$$

To proceed, the fractal-fractional coinfection COVID-19 and Zika virus model can be written as;

$$\begin{aligned}{}_0^{\mathbf{FFML}}D_{\varpi}^{c_1,c_2}\left(S_h^*(\varpi)\right)&=S_h^{*\ddot{\ddot{\ddot{}}}}\left(\varpi,S_h^*,I_C^{h*},I_Z^{h*},I_{CZ}^{h\ *},R^*,S_v^*,I_Z^{h*}\right),\\{}_0^{\mathbf{FFML}}D_{\varpi}^{c_1,c_2}\left(I_C^{h*}(\varpi)\right)&=I_C^{h\ddot{\ddot{\ddot{}}}}\left(\varpi,S_h^*,I_C^{h*},I_Z^{h*},I_{CZ}^{h\ *},R^*,S_v^*,I_Z^{h*}\right),\\{}_0^{\mathbf{FFML}}D_{\varpi}^{c_1,c_2}\left(I_Z^{h*}(\varpi)\right)&=I_Z^{h\ddot{\ddot{\ddot{}}}}\left(\varpi,S_h^*,I_C^{h*},I_Z^{h*},I_{CZ}^{h\ *},R^*,S_v^*,I_Z^{h*}\right),\\{}_0^{\mathbf{FFML}}D_{\varpi}^{c_1,c_2}\left(I_{CZ}^{h\ *}(\varpi)\right)&=I_{CZ}^{h\ \ddot{\ddot{\ddot{}}}}\left(\varpi,S_h^*,I_C^{h*},I_Z^{h*},I_{CZ}^{h\ *},R^*,S_v^*,I_Z^{h*}\right),\\{}_0^{\mathbf{FFML}}D_{\varpi}^{c_1,c_2}\left(R^*(\varpi)\right)&=R_T^{*\ddot{\ddot{\ddot{}}}}\left(\varpi,S_h^*,I_C^{h*},I_Z^{h*},I_{CZ}^{h\ *},R^*,S_v^*,I_Z^{h*}\right),\\{}_0^{\mathbf{FFML}}D_{\varpi}^{c_1,c_2}\left(S_v^*(\varpi)\right)&=S_v^{*\ddot{\ddot{\ddot{}}}}\left(\varpi,S_h^*,I_C^{h*},I_Z^{h*},I_{CZ}^{h\ *},R^*,S_v^*,I_Z^{h*}\right),\\{}_0^{\mathbf{FFML}}D_{\varpi}^{c_1,c_2}\left(S_v^*(\varpi)\right)&=I_Z^{v\ddot{\ddot{\ddot{}}}}\left(\varpi,S_h^*,I_C^{h*},I_Z^{h*},I_{CZ}^{h\ *},R^*,S_v^*,I_Z^{h*}\right).\end{aligned} \tag{44}$$

Using the above scheme in (43) the numerical scheme for fractal-fractional coinfection COVID-19 and Zika virus is written as;

$$\begin{aligned}S_h^{*p+1}=&S_{h_0}^*+\frac{(1-c_1)}{\mathbf{AB}(c_1)}c_2\varpi_p^{c_2-1}S_h^{*\ddot{\ddot{\ddot{}}}}\\&\left(\varpi_p,S_L^{*p},I_C^{h*p},I_Z^{h*p},I_{CZ}^{h\ *p},R^{*p},S_v^{*p},I_Z^{h*p}\right)+\frac{c_1h^{c_1}}{\mathbf{AB}(c_1)\Gamma(c_1+1)}\\&\sum_{q=2}^{p}c_2\varpi_{q-2}^{c_2-1}S_h^{*\ddot{\ddot{\ddot{}}}}\\&\left(\varpi_{q-2},S_L^{*q-2},I_C^{h*q-2},I_Z^{h*q-2},I_{CZ}^{h\ *q-2},R^{*q-2},S_v^{*q-2},I_Z^{h*q-2}\right)\\&\times\left[(p-q+1)^{c_1}-(p-q)^{c_1}\right]+\frac{c_1h^{c_1}}{\mathbf{AB}(c_1)\Gamma(c_1+2)}\\&\sum_{q=2}^{p}\begin{bmatrix}c_2\varpi_{q-1}^{c_2-1}S_h^{*\ddot{\ddot{\ddot{}}}}\left(\varpi_{q-1},S_L^{*q-1},I_C^{h*q-1},I_Z^{h*q-1},\right.\\I_{CZ}^{h\ *q-1},R^{*q-1},S_v^{*q-1},I_Z^{h*q-1}\left.\right)\\c_2\varpi_{q-2}^{c_2-1}S_h^{*\ddot{\ddot{\ddot{}}}}\left(\varpi_{q-2},S_L^{*q-2},I_C^{h*q-2},I_Z^{h*q-2},\right.\\I_{CZ}^{h\ *q-2},R^{*q-2},S_v^{*q-2},I_Z^{h*q-2}\left.\right)\end{bmatrix}\\&\times\begin{bmatrix}\left(p-q+1\right)^{c_1}\left(p-q+3+2c_1\right)\\-\left(p-q\right)^{c_1}\left(p-q+3+3c_1\right)\end{bmatrix}+\frac{c_1h^{c_1}}{2\mathbf{AB}(c_1)\Gamma(c_1+3)}\\&\sum_{q=2}^{p}\begin{bmatrix}c_2\varpi_q^{c_2-1}S_h^{*\ddot{\ddot{\ddot{}}}}\\\left(\varpi_q,S_L^{*q},I_C^{h*q},I_Z^{h*q},I_{CZ}^{h\ *q},R^{*q},S_v^{*q},I_Z^{h*q}\right)\\-2c_2\varpi_{q-1}^{c_2-1}S_h^{*\ddot{\ddot{\ddot{}}}}\left(\varpi_{q-1},S_L^{*q-1},I_C^{h*q-1},I_Z^{h*q-1},\right.\\I_{CZ}^{h\ *q-1},R^{*q-1},S_v^{*q-1},I_Z^{h*q-1}\left.\right)\\+c_2\varpi_{q-2}^{c_2-1}S_h^{*\ddot{\ddot{\ddot{}}}}\left(\varpi_{q-2},S_L^{*q-2},I_C^{h*q-2},I_Z^{h*q-2},\right.\\I_{CZ}^{h\ *q-2},R^{*q-2},S_v^{*q-2},I_Z^{h*q-2}\left.\right)\end{bmatrix}\\&\times\begin{bmatrix}\left(p-q+1\right)^{c_1}\left[2(p-q)^2+(3c_1-10)(p-q)+2c_1^2+9c_1+12\right]\\-\left(p-q\right)^{c_1}\left[2(p-q)^2+(5c_1-10)(p-q)+6c_1^2+18c_1+12\right]\end{bmatrix}.\end{aligned}$$

$$\begin{aligned}I_C^{h*p+1}=&I_{C0}^{h\ *}+\frac{(1-c_1)}{\mathbf{AB}(c_1)}c_2\varpi_p^{c_2-1}I_C^{h\ddot{\ddot{\ddot{}}}}\\&\left(\varpi_p,S_L^{*p},I_C^{h*p},I_Z^{h*p},I_{CZ}^{h\ *p},R^{*p},S_v^{*p},I_Z^{h*p}\right)\\&+\frac{c_1h^{c_1}}{\mathbf{AB}(c_1)\Gamma(c_1+1)}\\&\sum_{q=2}^{p}c_2\varpi_{q-2}^{c_2-1}I_C^{h\ddot{\ddot{\ddot{}}}}\\&\left(\varpi_{q-2},S_L^{*q-2},I_C^{h*q-2},I_Z^{h*q-2},I_{CZ}^{h\ *q-2},R^{*q-2},S_v^{*q-2},I_Z^{h*q-2}\right)\\&\times\left[(p-q+1)^{c_1}-(p-q)^{c_1}\right]\\&+\frac{c_1h^{c_1}}{\mathbf{AB}(c_1)\Gamma(c_1+2)}\end{aligned}$$

$$\sum_{q=2}^{p}\begin{bmatrix} c_2\varpi_{q-1}^{c_2-1} I_C^{h\,\ddot{*}}\left(\varpi_{q-1}, S_L^{*q-1}, I_C^{h*q-1}, I_Z^{h*q-1},\right. \\ \left. I_{CZ}^{h\ *q-1}, R^{*q-1}, S_v^{*q-1}, I_Z^{h*q-1}\right) \\ c_2\varpi_{q-2}^{c_2-1} I_C^{h\,\ddot{*}}\left(\varpi_{q-2}, S_L^{*q-2}, I_C^{h*q-2},\right. \\ \left. I_Z^{h*q-2}, I_{CZ}^{h\ *q-2}, R^{*q-2}, S_v^{*q-2}, I_Z^{h*q-2}\right) \end{bmatrix}$$
$$\times\begin{bmatrix} \left(p-q+1\right)^{c_1}\left(p-q+3+2c_1\right) \\ -\left(p-q\right)^{c_1}\left(p-q+3+3c_1\right) \end{bmatrix}$$
$$+\frac{c_1 h^{c_1}}{2\mathbf{AB}(c_1)\Gamma(c_1+3)}$$
$$\sum_{q=2}^{p}\begin{bmatrix} c_2\varpi_q^{c_2-1} I_C^{h\,\ddot{*}}\left(\varpi_q, S_L^{*q}, I_C^{h*q}, I_Z^{h*q},\right. \\ \left. I_{CZ}^{h\ *q}, R^{*q}, S_v^{*q}, I_Z^{h*q}\right) \\ -2c_2\varpi_{q-1}^{c_2-1} I_C^{h\,\ddot{*}}\left(\varpi_{q-1}, S_L^{*q-1}, I_C^{h*q-1}, I_Z^{h*q-1},\right. \\ \left. I_{CZ}^{h\ *q-1}, R^{*q-1}, S_v^{*q-1}, I_Z^{h*q-1}\right) \\ +c_2\varpi_{q-2}^{c_2-1} I_C^{h\,\ddot{*}}\left(\varpi_{q-2}, S_L^{*q-2}, I_C^{h*q-2}, I_Z^{h*q-2},\right. \\ \left. I_{CZ}^{h\ *q-2}, R^{*q-2}, S_v^{*q-2}, I_Z^{h*q-2}\right) \end{bmatrix}$$
$$\times\begin{bmatrix} \left(p-q+1\right)^{c_1}\left[2(p-q)^2+(3c_1-10)(p-q)+2c_1^2+9c_1+12\right] \\ -\left(p-q\right)^{c_1}\left[2(p-q)^2+(5c_1-10)(p-q)+6c_1^2+18c_1+12\right] \end{bmatrix}.$$

$$I_Z^{h\,*p+1} = I_{Z0}^{h\ *} + \frac{(1-c_1)}{\mathbf{AB}(c_1)} c_2\varpi_p^{c_2-1} I_Z^{h\,\ddot{*}}$$
$$\left(\varpi_p, S_L^{*p}, I_C^{h*p}, I_Z^{h*p}, I_{CZ}^{h\ *p}, R^{*p}, S_v^{*p}, I_Z^{h*p}\right)$$
$$+\frac{c_1 h^{c_1}}{\mathbf{AB}(c_1)\Gamma(c_1+1)}$$
$$\sum_{q=2}^{p} c_2\varpi_{q-2}^{c_2-1} I_Z^{h\,\ddot{*}}$$
$$\left(\varpi_{q-2}, S_L^{*q-2}, I_C^{h*q-2}, I_Z^{h*q-2}, I_{CZ}^{h\ *q-2}, R^{*q-2}, S_v^{*q-2}, I_Z^{h*q-2}\right)$$
$$\times\left[(p-q+1)^{c_1}-(p-q)^{c_1}\right]$$
$$+\frac{c_1 h^{c_1}}{\mathbf{AB}(c_1)\Gamma(c_1+2)}$$
$$\sum_{q=2}^{p}\begin{bmatrix} c_2\varpi_{q-1}^{c_2-1} I_Z^{h\,\ddot{*}}\left(\varpi_{q-1}, S_L^{*q-1}, I_C^{h*q-1}, I_Z^{h*q-1},\right. \\ \left. I_{CZ}^{h\ *q-1}, R^{*q-1}, S_v^{*q-1}, I_Z^{h*q-1}\right) \\ c_2\varpi_{q-2}^{c_2-1} I_Z^{h\,\ddot{*}}\left(\varpi_{q-2}, S_L^{*q-2}, I_C^{h*q-2}, I_Z^{h*q-2},\right. \\ \left. I_{CZ}^{h\ *q-2}, R^{*q-2}, S_v^{*q-2}, I_Z^{h*q-2}\right) \end{bmatrix}$$
$$\times\begin{bmatrix} \left(p-q+1\right)^{c_1}\left(p-q+3+2c_1\right) \\ -\left(p-q\right)^{c_1}\left(p-q+3+3c_1\right) \end{bmatrix}$$
$$+\frac{c_1 h^{c_1}}{2\mathbf{AB}(c_1)\Gamma(c_1+3)}$$
$$\sum_{q=2}^{p}\begin{bmatrix} c_2\varpi_q^{c_2-1} I_Z^{h\,\ddot{*}}\left(\varpi_q, S_L^{*q}, I_C^{h*q}, I_Z^{h*q},\right. \\ \left. I_{CZ}^{h\ *q}, R^{*q}, S_v^{*q}, I_Z^{h*q}\right) \\ -2c_2\varpi_{q-1}^{c_2-1} I_Z^{h\,\ddot{*}}\left(\varpi_{q-1}, S_L^{*q-1}, I_C^{h*q-1}, I_Z^{h*q-1},\right. \\ \left. I_{CZ}^{h\ *q-1}, R^{*q-1}, S_v^{*q-1}, I_Z^{h*q-1}\right) \\ +c_2\varpi_{q-2}^{c_2-1} I_Z^{h\,\ddot{*}}\left(\varpi_{q-2}, S_L^{*q-2}, I_C^{h*q-2}, I_Z^{h*q-2},\right. \\ \left. I_{CZ}^{h\ *q-2}, R^{*q-2}, S_v^{*q-2}, I_Z^{h*q-2}\right) \end{bmatrix}$$
$$\times\begin{bmatrix} \left(p-q+1\right)^{c_1}\left[2(p-q)^2+(3c_1-10)(p-q)+2c_1^2+9c_1+12\right] \\ -\left(p-q\right)^{c_1}\left[2(p-q)^2+(5c_1-10)(p-q)+6c_1^2+18c_1+12\right] \end{bmatrix}.$$

$$I_{CZ}^{h\ *p+1} = I_{CZ0}^{h\ *} + \frac{(1-c_1)}{\mathbf{AB}(c_1)} c_2\varpi_p^{c_2-1} I_{CZ}^{h\ \ddot{*}}$$
$$\left(\varpi_p, S_L^{*p}, I_C^{h*p}, I_Z^{h*p}, I_{CZ}^{h\ *p}, R^{*p}, S_v^{*p}, I_Z^{h*p}\right)$$
$$+\frac{c_1 h^{c_1}}{\mathbf{AB}(c_1)\Gamma(c_1+1)}$$
$$\sum_{q=2}^{p} c_2\varpi_{q-2}^{c_2-1} I_{CZ}^{h\ \ddot{*}}$$
$$\left(\varpi_{q-2}, S_L^{*q-2}, I_C^{h*q-2}, I_Z^{h*q-2}, I_{CZ}^{h\ *q-2}, R^{*q-2}, S_v^{*q-2}, I_Z^{h*q-2}\right)$$
$$\times\left[(p-q+1)^{c_1}-(p-q)^{c_1}\right]$$
$$+\frac{c_1 h^{c_1}}{\mathbf{AB}(c_1)\Gamma(c_1+2)}$$
$$\sum_{q=2}^{p}\begin{bmatrix} c_2\varpi_{q-1}^{c_2-1} I_{CZ}^{h\ \ddot{*}}\left(\varpi_{q-1}, S_L^{*q-1}, I_C^{h*q-1}, I_Z^{h*q-1},\right. \\ \left. I_{CZ}^{h\ *q-1}, R^{*q-1}, S_v^{*q-1}, I_Z^{h*q-1}\right) \\ c_2\varpi_{q-2}^{c_2-1} I_{CZ}^{h\ \ddot{*}}\left(\varpi_{q-2}, S_L^{*q-2}, I_C^{h*q-2}, I_Z^{h*q-2},\right. \\ \left. I_{CZ}^{h\ *q-2}, R^{*q-2}, S_v^{*q-2}, I_Z^{h*q-2}\right) \end{bmatrix}$$
$$\times\begin{bmatrix} \left(p-q+1\right)^{c_1}\left(p-q+3+2c_1\right) \\ -\left(p-q\right)^{c_1}\left(p-q+3+3c_1\right) \end{bmatrix}$$
$$+\frac{c_1 h^{c_1}}{2\mathbf{AB}(c_1)\Gamma(c_1+3)}$$
$$\sum_{q=2}^{p}\begin{bmatrix} c_2\varpi_q^{c_2-1} I_{CZ}^{h\ \ddot{*}}\left(\varpi_q, S_L^{*q}, I_C^{h*q}, I_Z^{h*q},\right. \\ \left. I_{CZ}^{h\ *q}, R^{*q}, S_v^{*q}, I_Z^{h*q}\right) \\ -2c_2\varpi_{q-1}^{c_2-1} I_{CZ}^{h\ \ddot{*}}\left(\varpi_{q-1}, S_L^{*q-1}, I_C^{h*q-1}, I_Z^{h*q-1},\right. \\ \left. I_{CZ}^{h\ *q-1}, R^{*q-1}, S_v^{*q-1}, I_Z^{h*q-1}\right) \\ +c_2\varpi_{q-2}^{c_2-1} I_{CZ}^{h\ \ddot{*}}\left(\varpi_{q-2}, S_L^{*q-2}, I_C^{h*q-2}, I_Z^{h*q-2},\right. \\ \left. I_{CZ}^{h\ *q-2}, R^{*q-2}, S_v^{*q-2}, I_Z^{h*q-2}\right) \end{bmatrix}$$
$$\times\begin{bmatrix} \left(p-q+1\right)^{c_1}\left[2(p-q)^2+(3c_1-10)(p-q)+2c_1^2+9c_1+12\right] \\ -\left(p-q\right)^{c_1}\left[2(p-q)^2+(5c_1-10)(p-q)+6c_1^2+18c_1+12\right] \end{bmatrix}.$$

$$R^{*p+1} = R_0^{\ *} + \frac{(1-c_1)}{\mathbf{AB}(c_1)} c_2\varpi_p^{c_2-1} R^{\ddot{*}}$$
$$\left(\varpi_p, S_L^{*p}, I_C^{h*p}, I_Z^{h*p}, I_{CZ}^{h\ *p}, R^{*p}, S_v^{*p}, I_Z^{h*p}\right)$$
$$+\frac{c_1 h^{c_1}}{\mathbf{AB}(c_1)\Gamma(c_1+1)}$$
$$\sum_{q=2}^{p} c_2\varpi_{q-2}^{c_2-1} R^{\ddot{*}}$$
$$\left(\varpi_{q-2}, S_L^{*q-2}, I_C^{h*q-2}, I_Z^{h*q-2}, I_{CZ}^{h\ *q-2}, R^{*q-2}, S_v^{*q-2}, I_Z^{h*q-2}\right)$$
$$\times\left[(p-q+1)^{c_1}-(p-q)^{c_1}\right]$$
$$+\frac{c_1 h^{c_1}}{\mathbf{AB}(c_1)\Gamma(c_1+2)}$$
$$\sum_{q=2}^{p}\begin{bmatrix} c_2\varpi_{q-1}^{c_2-1} R^{\ddot{*}}\left(\varpi_{q-1}, S_L^{*q-1}, I_C^{h*q-1}, I_Z^{h*q-1},\right. \\ \left. I_{CZ}^{h\ *q-1}, R^{*q-1}, S_v^{*q-1}, I_Z^{h*q-1}\right) \\ c_2\varpi_{q-2}^{c_2-1} R^{\ddot{*}}\left(\varpi_{q-2}, S_L^{*q-2}, I_C^{h*q-2}, I_Z^{h*q-2},\right. \\ \left. I_{CZ}^{h\ *q-2}, R^{*q-2}, S_v^{*q-2}, I_Z^{h*q-2}\right) \end{bmatrix}$$
$$\times\begin{bmatrix} \left(p-q+1\right)^{c_1}\left(p-q+3+2c_1\right) \\ -\left(p-q\right)^{c_1}\left(p-q+3+3c_1\right) \end{bmatrix}$$
$$+\frac{c_1 h^{c_1}}{2\mathbf{AB}(c_1)\Gamma(c_1+3)}$$
$$\sum_{q=2}^{p}\begin{bmatrix} c_2\varpi_q^{c_2-1} R^{\ddot{*}}\left(\varpi_q, S_L^{*q}, I_C^{h*q}, I_Z^{h*q}, I_{CZ}^{h\ *q}, R^{*q}, S_v^{*q}, I_Z^{h*q}\right) \\ -2c_2\varpi_{q-1}^{c_2-1} R^{\ddot{*}}\left(\varpi_{q-1}, S_L^{*q-1}, I_C^{h*q-1}, I_Z^{h*q-1},\right. \\ \left. I_{CZ}^{h\ *q-1}, R^{*q-1}, S_v^{*q-1}, I_Z^{h*q-1}\right) \\ +c_2\varpi_{q-2}^{c_2-1} R^{\ddot{*}}\left(\varpi_{q-2}, S_L^{*q-2}, I_C^{h*q-2}, I_Z^{h*q-2},\right. \\ \left. I_{CZ}^{h\ *q-2}, R^{*q-2}, S_v^{*q-2}, I_Z^{h*q-2}\right) \end{bmatrix}$$
$$\times\begin{bmatrix} \left(p-q+1\right)^{c_1}\left[2(p-q)^2+(3c_1-10)(p-q)+2c_1^2+9c_1+12\right] \\ -\left(p-q\right)^{c_1}\left[2(p-q)^2+(5c_1-10)(p-q)+6c_1^2+18c_1+12\right] \end{bmatrix}.$$

$$S_v^{\ *p+1} = S_{v0}^{\ *} + \frac{(1-c_1)}{\mathbf{AB}(c_1)} c_2\varpi_p^{c_2-1} S_v^{\ddot{*}}$$
$$\left(\varpi_p, S_L^{*p}, I_C^{h*p}, I_Z^{h*p}, I_{CZ}^{h\ *p}, R^{*p}, S_v^{*p}, I_Z^{h*p}\right)$$

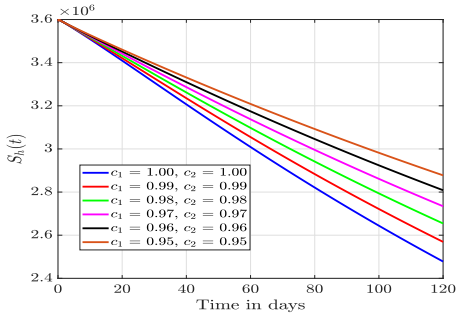

(a) Fractal-fractional solution profile of susceptibles

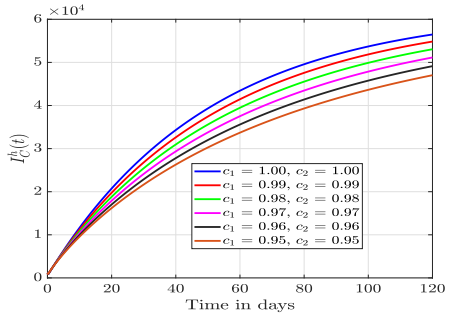

(b) Fractal-fractional solution profile of infectious COVID-19 humans

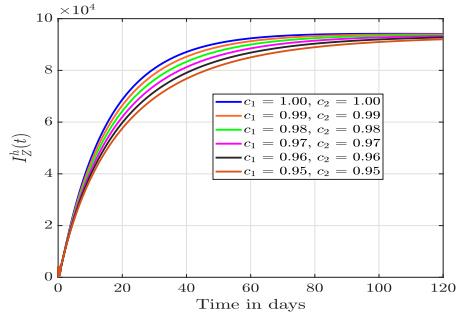

(c) Fractal-fractional solution profile of infectious humans with Zika

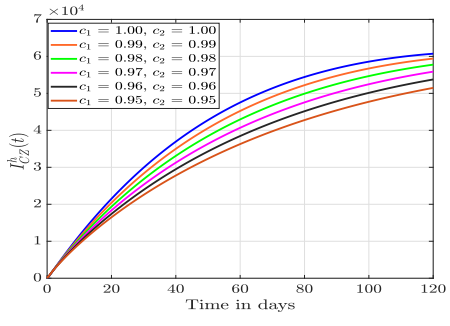

(d) Fractal-fractional solution profile of infectious humans with COVID-19 and Zika

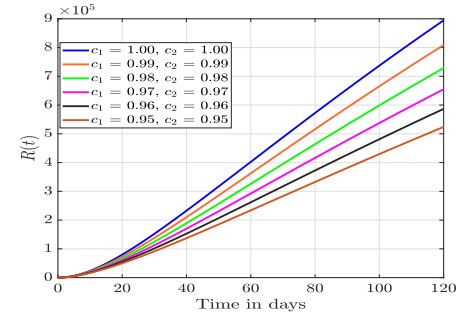

(e) Fractal-fractional solution profile of recovered humans

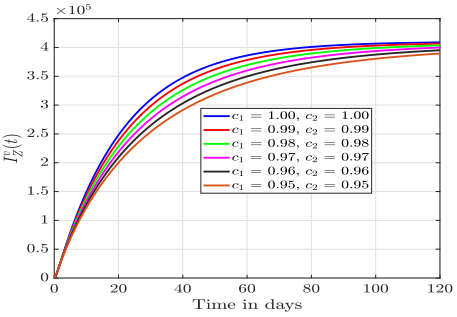

(f) Fractal-fractional solution profile of infectious vectors

Fig. 1. Numerical simulation under hybrid derivative with change in both fractal dimension and fractional order, $c_1 = c_2 = 0.99, 0.98, 0.97, 0.96, 0.95$.

$$
\begin{aligned}
&+\frac{c_1 h^{c_1}}{\mathbf{AB}(c_1)\Gamma(c_1+1)}\\
&\sum_{q=2}^{p} c_2 \varpi_{q-2}^{c_2-1} S_v^{\ast\ast\ast}\\
&\left(\varpi_{q-2}, S_L^{*q-2}, I_C^{h\,*q-2}, I_Z^{h\,*q-2}, I_{CZ}^{h\ *q-2}, R^{*q-2}, S_v^{\ *q-2}, I_Z^{h\,*q-2}\right)\\
&\times\left[(p-q+1)^{c_1}-(p-q)^{c_1}\right]\\
&+\frac{c_1 h^{c_1}}{\mathbf{AB}(c_1)\Gamma(c_1+2)}\\
&\sum_{q=2}^{p}\begin{bmatrix} c_2\varpi_{q-1}^{c_2-1} S_v^{\ast\ast\ast}\left(\varpi_{q-1}, S_L^{*q-1}, I_C^{h\,*q-1}, I_Z^{h\,*q-1},\right.\\ \left. I_{CZ}^{h\ *q-1}, R^{*q-1}, S_v^{\ *q-1}, I_Z^{h\,*q-1}\right)\\ c_2\varpi_{q-2}^{c_2-1} S_v^{\ast\ast\ast}\left(\varpi_{q-2}, S_L^{*q-2}, I_C^{h\,*q-2}, I_Z^{h\,*q-2},\right.\\ \left. I_{CZ}^{h\ *q-2}, R^{*q-2}, S_v^{\ *q-2}, I_Z^{h\,*q-2}\right)\end{bmatrix}\\
&\times\begin{bmatrix}\left(p-q+1\right)^{c_1}\left(p-q+3+2c_1\right)\\ -\left(p-q\right)^{c_1}\left(p-q+3+3c_1\right)\end{bmatrix}\\
&+\frac{c_1 h^{c_1}}{2\mathbf{AB}(c_1)\Gamma(c_1+3)}\\
&\sum_{q=2}^{p}\begin{bmatrix} c_2\varpi_q^{c_2-1} S_v^{\ast\ast\ast}\\ \left(\varpi_q, S_L^{*q}, I_C^{h\,*q}, I_Z^{h\,*q}, I_{CZ}^{h\ *q}, R^{*q}, S_v^{\ *q}, I_Z^{h\,*q}\right)\\ -2c_2\varpi_{q-1}^{c_2-1} S_v^{\ast\ast\ast}\left(\varpi_{q-1}, S_L^{*q-1}, I_C^{h\,*q-1}, I_Z^{h\,*q-1},\right.\\ \left. I_{CZ}^{h\ *q-1}, R^{*q-1}, S_v^{\ *q-1}, I_Z^{h\,*q-1}\right)\\ +c_2\varpi_{q-2}^{c_2-1} S_v^{\ast\ast\ast}\left(\varpi_{q-2}, S_L^{*q-2}, I_C^{h\,*q-2}, I_Z^{h\,*q-2},\right.\\ \left. I_{CZ}^{h\ *q-2}, R^{*q-2}, S_v^{\ *q-2}, I_Z^{h\,*q-2}\right)\end{bmatrix}\\
&\times\begin{bmatrix}\left(p-q+1\right)^{c_1}\left[2(p-q)^2+(3c_1-10)(p-q)+2c_1^2+9c_1+12\right]\\ -\left(p-q\right)^{c_1}\left[2(p-q)^2+(5c_1-10)(p-q)+6c_1^2+18c_1+12\right]\end{bmatrix}.
\end{aligned}
$$

$$
\begin{aligned}
I_Z^{v\,*p+1} =& I_{Z0}^{v\ *}+\frac{(1-c_1)}{\mathbf{AB}(c_1)} c_2\varpi_p^{c_2-1} I_v^{h\ast\ast}\\
&\left(\varpi_p, S_L^{*p}, I_C^{h\,*p}, I_Z^{h\,*p}, I_{CZ}^{h\ *p}, R^{*p}, S_v^{\ *p}, I_Z^{h\,*p}\right)\\
&+\frac{c_1 h^{c_1}}{\mathbf{AB}(c_1)\Gamma(c_1+1)}\\
&\sum_{q=2}^{p} c_2\varpi_{q-2}^{c_2-1} I_v^{h\ast\ast}\\
&\left(\varpi_{q-2}, S_L^{*q-2}, I_C^{h\,*q-2}, I_Z^{h\,*q-2}, I_{CZ}^{h\ *q-2}, R^{*q-2}, S_v^{\ *q-2}, I_Z^{h\,*q-2}\right)
\end{aligned}
$$

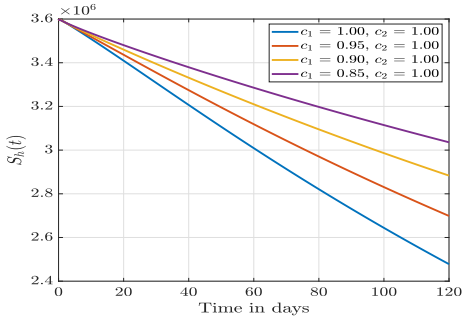

(a) Fractional solution profile of susceptibles

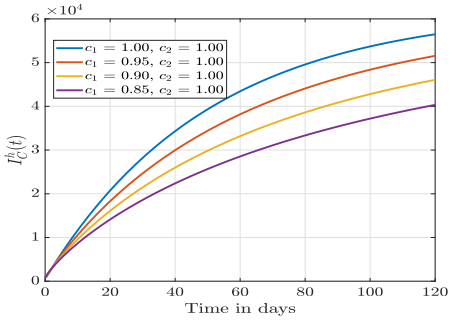

(b) Fractional solution profile of infectious COVID-19 humans

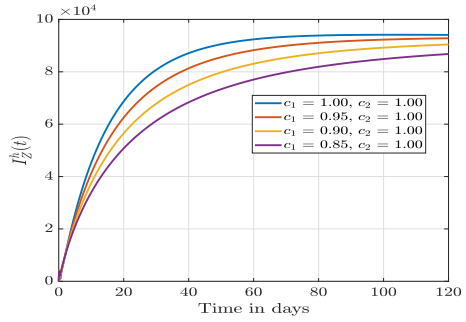

(c) Fractional solution profile of infectious humans with Zika

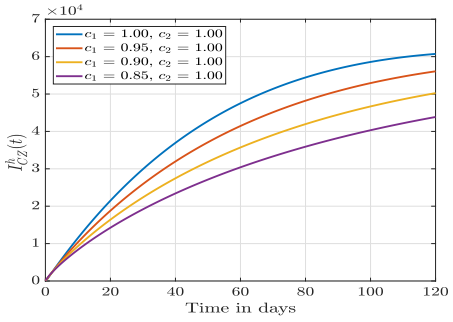

(d) Fractional solution profile of infectious humans with COVID-19 and Zika

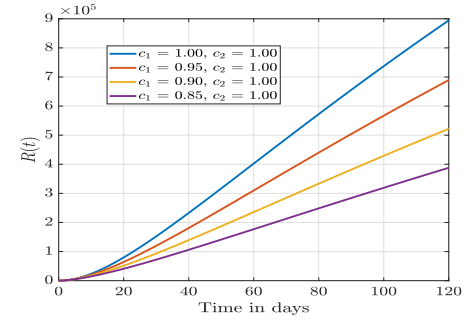

(e) Fractional solution profile of recovered humans

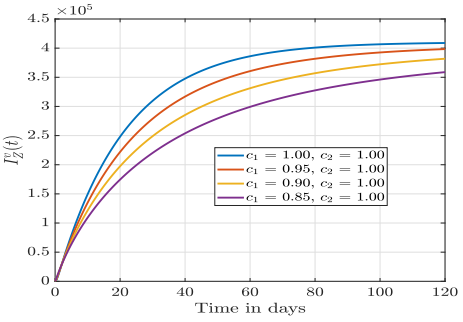

(f) Fractional solution profile of infectious vectors

Fig. 2. Numerical simulation under hybrid derivative with fractional order $c_1 = 1.00, 0.95, 0.90, 0.85$, with constant fractal dimension.

$$\times\left[(p-q+1)^{c_1}-(p-q)^{c_1}\right]$$
$$+\frac{c_1 h^{c_1}}{\mathbf{AB}(c_1)\Gamma(c_1+2)}$$
$$\sum_{q=2}^{p}\begin{bmatrix} c_2\varpi_{q-1}^{c_2-1} I_v^{h\,\ddot{*}}\left(\varpi_{q-1}, S_L^{*q-1}, I_C^{h\,*q-1}, I_Z^{h\,*q-1},\right. \\ \left. I_{CZ}^{h\ *q-1}, R^{*q-1}, S_v^{*q-1}, I_Z^{h\,*q-1}\right) \\ c_2\varpi_{q-2}^{c_2-1} I_v^{h\,\ddot{*}}\left(\varpi_{q-2}, S_L^{*q-2}, I_C^{h\,*q-2}, I_Z^{h\,*q-2},\right. \\ \left. I_{CZ}^{h\ *q-2}, R^{*q-2}, S_v^{*q-2}, I_Z^{h\,*q-2}\right)\end{bmatrix}$$
$$\times\begin{bmatrix}\left(p-q+1\right)^{c_1}\left(p-q+3+2c_1\right) \\ -\left(p-q\right)^{c_1}\left(p-q+3+3c_1\right)\end{bmatrix}$$
$$+\frac{c_1 h^{c_1}}{2\mathbf{AB}(c_1)\Gamma(c_1+3)}$$
$$\sum_{q=2}^{p}\begin{bmatrix} c_2\varpi_q^{c_2-1} I_v^{h\,\ddot{*}} \\ \left(\varpi_q, S_L^{*q}, I_C^{h\,*q}, I_Z^{h\,*q}, I_{CZ}^{h\ *q}, R^{*q}, S_v^{\ *q}, I_Z^{h\,*q}\right) \\ -2c_2\varpi_{q-1}^{c_2-1} I_v^{h\,\ddot{*}}\left(\varpi_{q-1}, S_L^{*q-1}, I_C^{h\,*q-1}, I_Z^{h\,*q-1},\right. \\ \left. I_{CZ}^{h\ *q-1}, R^{*q-1}, S_v^{*q-1}, I_Z^{h\,*q-1}\right) \\ +c_2\varpi_{q-2}^{c_2-1} I_v^{h\,\ddot{*}}\left(\varpi_{q-2}, S_L^{*q-2},\right. \\ \left. I_C^{h\,*q-2}, I_Z^{h\,*q-2}, I_{CZ}^{h\ *q-2}, R^{*q-2}, S_v^{\ *q-2}, I_Z^{h\,*q-2}\right)\end{bmatrix}$$
$$\times\begin{bmatrix}\left(p-q+1\right)^{c_1}\left[2(p-q)^2+(3c_1-10)(p-q)+2c_1^2+9c_1+12\right] \\ -\left(p-q\right)^{c_1}\left[2(p-q)^2+(5c_1-10)(p-q)+6c_1^2+18c_1+12\right]\end{bmatrix}.$$

Simulations and discussion

The numerical results of our work, which comprise both solution routes for each compartment and a change in some parameters under the fractal-fractional model, are discussed in this part. The Newton polynomial-based numerical iterative system in Section i is used to simulate the nonlinear fractal-fractional deterministic model. The numerical solutions or trajectories of the newly created fractal-fractional model were derived using the initial conditions $S_h(0) = 3\,600\,000$, $I_C^h(0) = 800$, $I_Z^h(0) = 24$, $I_{CZ}^h(0) = 100$, $R(0) = 100$, $S_v(0) = 4000$, $I_z^v(0) = 600$ for this purpose, with time step $h = 0.12$. Furthermore, the parameter values used can be found in Table 2.

Fig. 1 shows the numerical output of the proposed fractal-fractional model when both the fractal dimension and the fractional order are varied simultaneously. It is noticed that a reduction in the fractal-fractional orders captures different roles of memory effects on the dynamics of disease spread. It is evident that the number of infected humans with COVID-19 only, infected humans with Zika virus only,

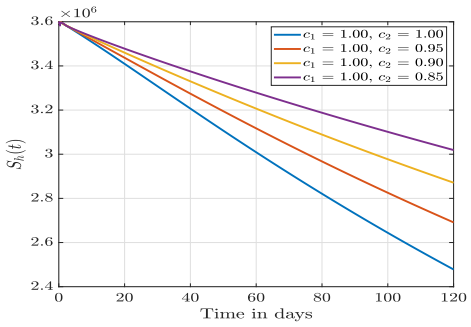

(a) Fractal solution profile of susceptibles

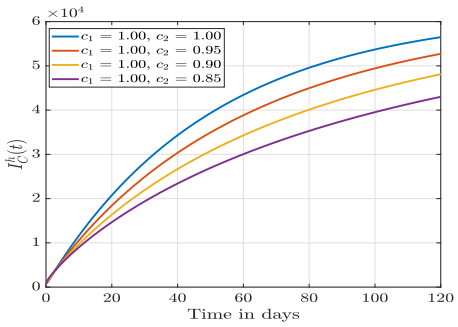

(b) Fractal solution profile of infectious humans with COVID-19

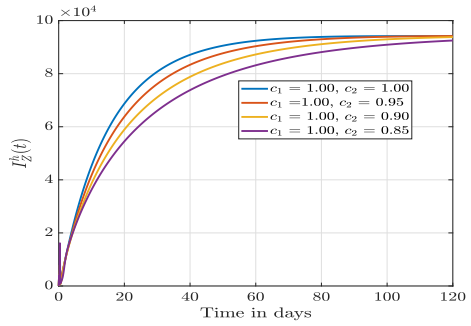

(c) Fractal solution profile of infectious humans with Zika

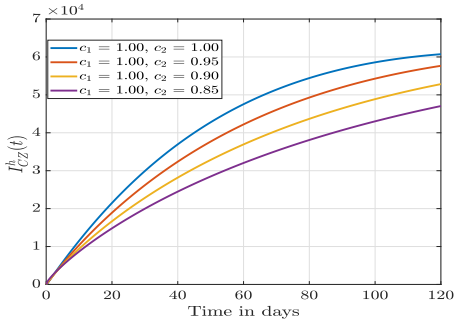

(d) Fractal solution profile of infectious humans with COVID-19 and Zika

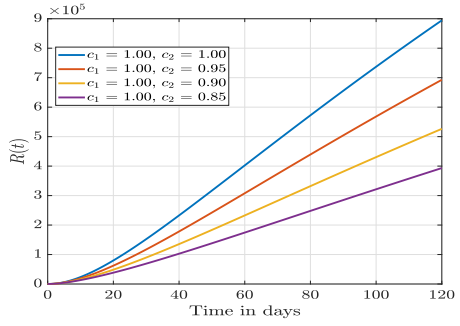

(e) Fractal solution profile of recovered humans

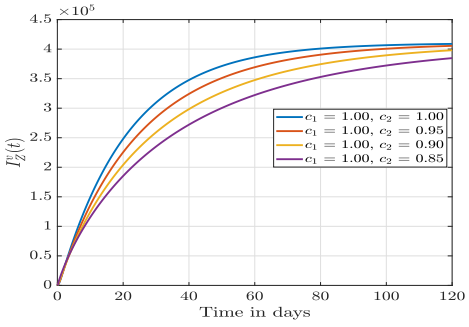

(f) Fractal solution profile of infectious vectors

Fig. 3. Numerical simulation under hybrid derivative with constant fractional order and fractal dimension $c_2 = 0.95, 0.90, 0.85$.

infected humans with COVID-19 and Zika virus, recovered humans and infectious vectors reduces as the fractal-fractional order reduces, while that of susceptible humans increases. The dynamic of the susceptible vector shows no trajectory effect, so we did not show it here. Furthermore, it is noticed that the compartmental trajectories of infected humans with Zika virus and infected vectors with Zika virus move to the same converging point as time increases.

Fig. 2 gives the virous numerical graphs when the fractional order is kept at the integer order and one has the choice to vary the fractal order only. It is observed that a fractal difference of 0.5 between each fractal step results in different asymptotic stability for all compartmental classes; however, there is no new visible difference in the susceptible vectors, so it is not shown here.

Fig. 3 shows the interesting numerical graphs when the fractal order is kept constant and only the fractional order is varied. It is discovered that a fractional difference of 0.5 between each fractional step results in different asymptotic stability for susceptible humans, infected humans with COVID-19 alone, infected humans with COVID-19 and Zika, and recovered humans, whereas infectious humans and infectious vectors with Zika only converge to the same stability as time increases.

Figs. 4 and 5(a) show that simulation impacts have varying saturating effects on the proposed model. It is noticed that the inclusion of this function gives a unique memory effect of the transmission of the coinfection model of COVID-19 and Zika. Thus, an increase in the saturating effect increases the number of healthy individuals and susceptible vectors, with a reduction in the number of infected and recovered individuals. Figs. 5(b)–5(f) shows the impact of the effective contact rate for human-to-human transmission of COVID-19 on the model. It is noticed that an increase in the effective contact rate for human to human transmission of COVID-19 reduces the number of susceptible humans, increases the number of infectious humans with COVID-19 only, has no significant effect on the number of infected humans with Zika only, and causes an increase in the number of infectious humans with both COVID-19 and Zika virus after 37 days and a slight reduction in the number of recovered humans.

Figs. 6(a)–6(d) show the dynamical effectiveness of the contact rate for human-to-human transmission of Zika in the proposed model. From

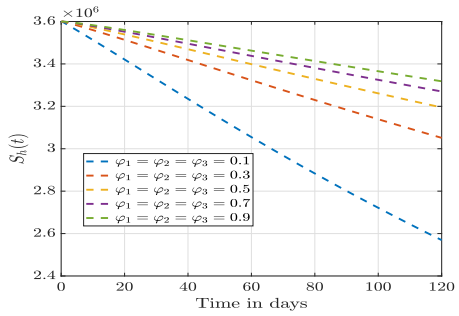

(a) Varying the saturating effects on susceptible humans.

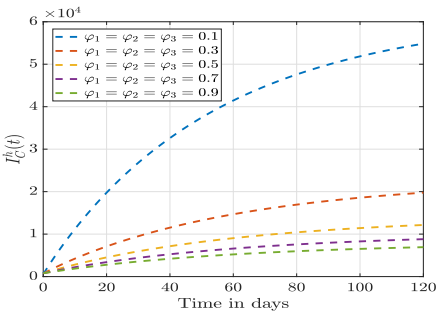

(b) Varying saturating effects on infectious humans with COVID-19 .

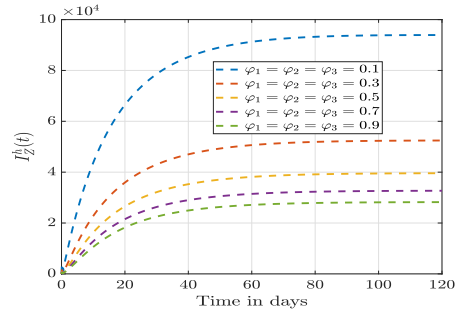

(c) Varying saturating effects on infectious humans with Zika virus.

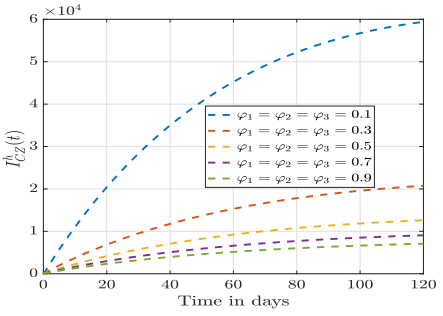

(d) Varying saturating effects on humans co-infected with COVID- 19 and Zika virus.

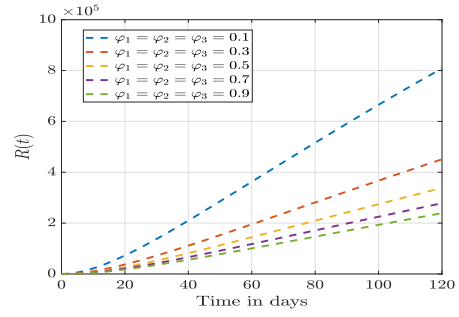

(e) Varying saturating effects on recovered from COVID-19 and Zika virus.

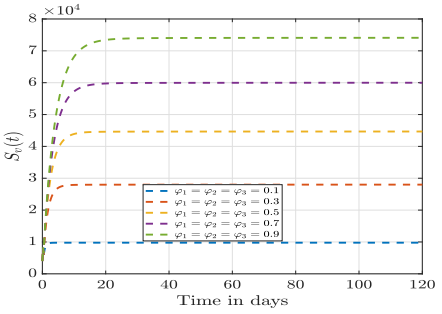

(f) Varying saturating effects on susceptible vectors.

Fig. 4. Numerical simulation under hybrid derivative with fractal-fractional order of 0.99.

this simulation, it is noticed that an increase in the effective contact rate for human to human transmission of Zika reduces the number of susceptible humans, increases the number of infectious humans with COVID-19 only, shows a significant increase in the number of infected humans with Zika only, shows a slight reduction in the number of recovered humans and no increase in the number of infectious humans with both COVID-19 and Zika virus, hence we did not show it here.

Figs. 6(e), 6(f) and Figs. 7(a)–7(c) show the dynamical effect of contact rate on co-infection transmission in the proposed model. It is noticed from this simulation that an increase in the effective contact rate for co-infection transmission reduces the number of susceptible humans. There is no increase in the number of infectious humans with COVID-19 only, no increase in the number of infected humans with Zika only, but a significant increase in the number of infectious humans with both COVID-19 and Zika, and a slight increase in the number of recovered humans. The numerical dynamics of varying the effective contact rate for vector to human transmission of Zika is shown in Figs. 7(d) and 8(b). It is noticed that an increase in the effective contact rate for vector to human transmission of Zika reduces the number of susceptibles and increases the number of infected humans with COVID-19 and the number of infected humans with Zika virus only slightly more than the other effective contact rates considered here.

Fig. 8(a) shows the dynamics of varying effective contact rates for vector-to-human transmission of Zika on the coinfection compartment. It is seen that increasing this rate does not have any significant change during the initial days of infection until the 100th day. Fig. 8(b) clearly shows that the rate of change in the vector to human transmission of Zika directly reduces the number of recovered individuals. After a numerical simulation on the effective contact rate for human to vector transmission of Zika, it was noticed that the rate of change of the effective contact rate for human to vector transmission of Zika does not give a trajectory change in the compartmental dynamics, so it was not shown here.

The trajectory change of the modification parameter of transmission is depicted in Fig. 8(c) and Fig. 8(d). It is noticed that a reduction in the modification parameter of transmission only affects the number of individuals infected with COVID-19 and the Zika virus only after the 60th day, respectively.

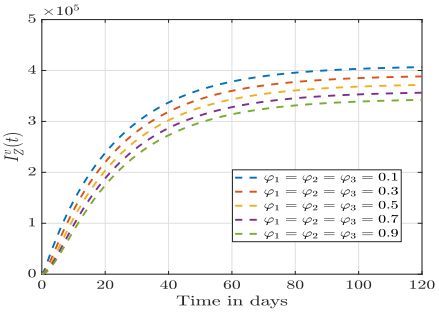

(a) Varying saturating effects on vectors infected with Zika virus.

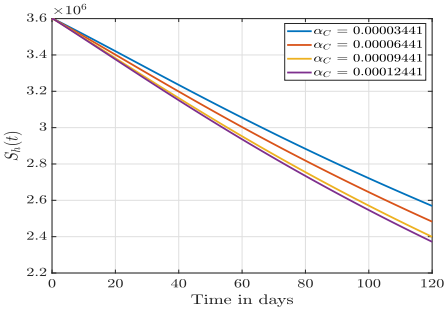

(b) Varying effective contact rate for human-human transmission of COVID-19 on susceptible humans

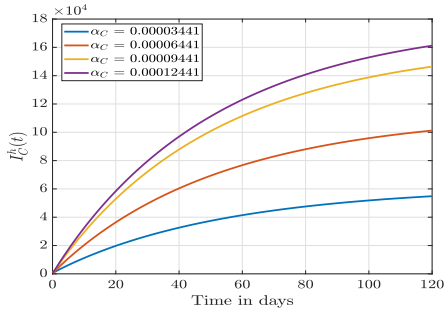

(c) Varying effective contact rate for human-human transmission of COVID-19 on infectious humans with COVID-19.

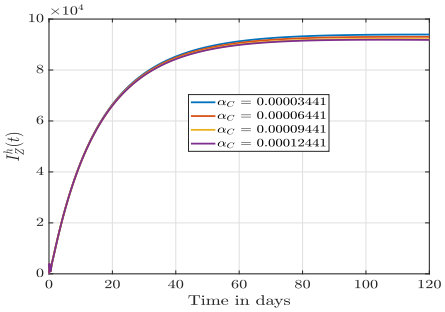

(d) Varying effective contact rate for human-human transmission of COVID-19 on infectious humans with Zika.

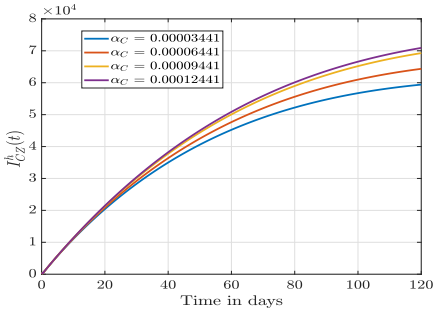

(e) Varying effective contact rate for human-human transmission of COVID-19 on co-infection individuals

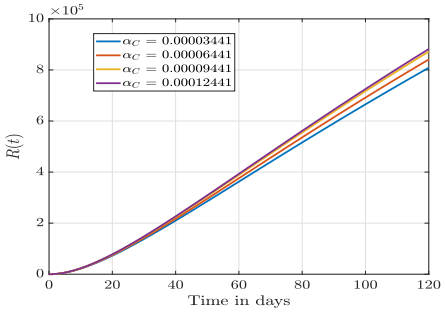

(f) Varying the effective contact rate for human-human transmission of COVID-19 on recovered humans.

Fig. 5. Numerical simulation under hybrid derivative with fractal-fractional order of 0.99.

Table 2
Values in the fractal-fractional hybrid model (13).

Parameter	Value	References
Ψ^h	$\frac{4108508}{74.9\times 365}$ per day	[63]
Ψ^v	20,000 per day	[64]
α_C	0.00003441	Assumed
α_Z	0.000035	Assumed
α_{CZ}	0.000035	Assumed
α_Z^h	0.00005	Assumed
α_Z^v	0.2	Assumed
ϱ_h	$\frac{1}{74.9\times 365}$ per day	[65]
ϱ_v	$\frac{1}{21}$ per day	[64]
ζ_1, ζ_2	1.0	Assumed
ϑ_1, ϑ_2	1.0	Assumed
$\delta_C, \delta_Z, \delta_{CZ}$	0.001	[64]
γ_C	0.015	[10]
γ_Z	0.09–0.15	[60]
γ_{CZ}	0.015	Assumed
$\varphi_1, \varphi_2, \varphi_3$	0.1–0.65	[58]

Finally, this study looks at the relative impact of the rate of re-infection with COVID-19 or Zika in Fig. 8(e) and Fig. 8(f). It is noticed that the rate of re-infection with COVID-19 has a small impact on the number of humans infected with COVID-19 only and the number of humans with both COVID-19 and Zika. The change in the re-infection rate of humans with Zika shows no trajectory change in our proposed model.

Conclusion

Given the recent emergence of fractal-fractional operators in scholarly discourse, their application in investigating the intricate mathematical patterns of co-infections involving diverse diseases remains unexplored. It is important to acknowledge that our study represents the initial investigation into the co-infection phenomenon within the framework of the fractal-fractional model utilizing the Mittag-Leffler hybrid kernel. That is, a new two-parametric fractal-fractional Mittag-Leffler hybrid model for COVID-19 and Zika co-dynamics was designed and studied to evaluate the impact of COVID-19 on Zika and vice-versa. The local and global stability analysis were carried out for the standard model based on the obtained basic reproduction number. The existence and uniqueness are two important properties that we

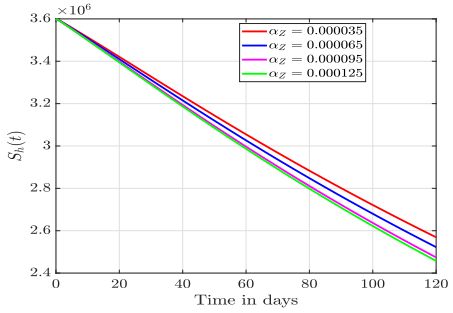

(a) varying effective contact rate for human-human transmission of Zika on susceptible humans

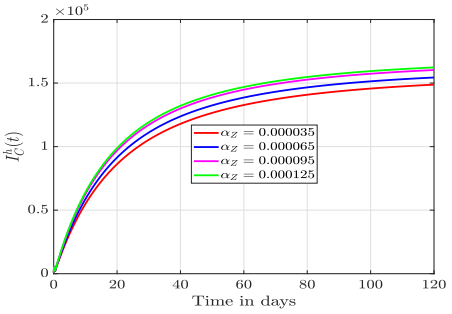

(b) Varying effective contact rate for human-human transmission of Zika on infectious humans with COVID-19

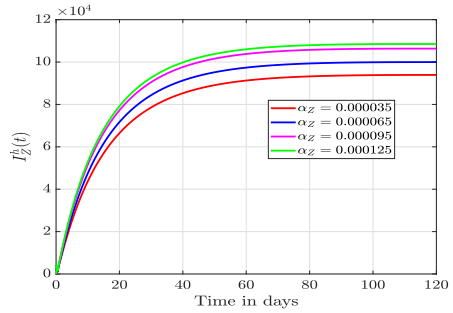

(c) Varying effective contact rate for human-human transmission of Zika on infectious humans with Zika

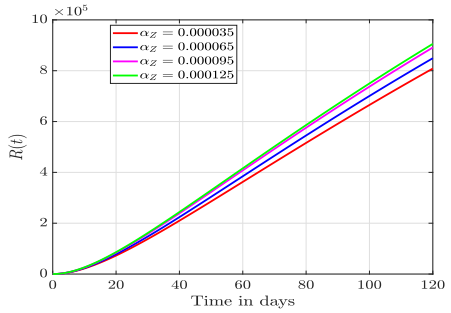

(d) The of varying effective contact rate for human-human transmission of Zika on recovered humans.

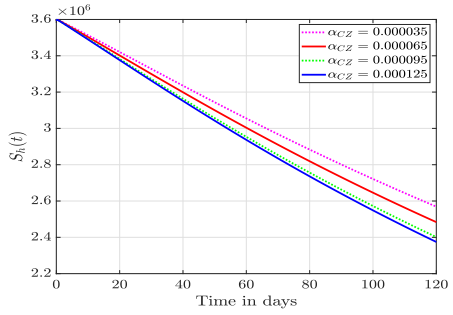

(e) Varying effective contact rate for co-infection transmission on susceptible humans.

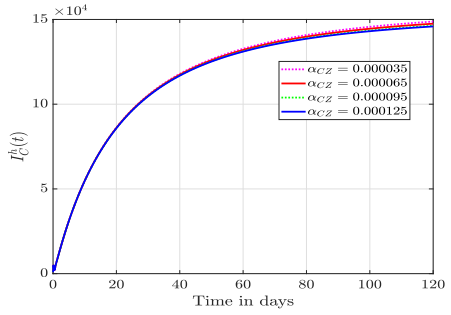

(f) Varying effective contact rate for co-infection transmission on infectious humans with COVID-19.

Fig. 6. Numerical simulation under hybrid derivative with fractal-fractional order of 0.99.

proved them via the fixed-point's tools. Also, stable solutions were investigated according to Ulam's criterion. With the help of the Newton polynomials, we produced a numerical scheme for each solution of the fractal-fractional system of integral equations and dioscussed the relevant results based on numerical simulations obtained by given real data. We also assessed the role of two parameters of fractional order and fractal dimension in the final outcomes of simulations. We analyzed the dynamical behavior of each solution completely in some graphs and found that the prevention of the spread of the SARS-CoV-2 virus has a high positive effect on reducing co-infections with Zika. The effects of fractional and fractal orders on epidemiological class dynamics are also examined. Thus, healthcare systems must constantly monitor for abnormal patterns or co-infections, especially in places where both diseases are prevalent. Since our understanding of diseases may evolve, it is important to consult the latest health authority guidelines.

Funding

No funds were received.

CRediT authorship contribution statement

Shahram Rezapour: Conceptualization. **Joshua Kiddy K. Asamoah:** Conceptualization, Investigation, Data curation, Writing - review and editing. **Sina Etemad:** Formal analysis. **Ali Akgül:** Investigation. **İbrahim Avcı:** Methodology. **Sayed M. El Din:** Conceptualization, Investigation, Supervision.

Data availability

No data was used for the research described in the article.

Acknowledgments

The first and third authors would like to thank Azarbaijan Shahid Madani University. Also, all authors would like to thank dear reviewers for their constructive comments to improve the quality of the paper.

Declaration of competing interest

The authors declare that they have no conflict of interest.

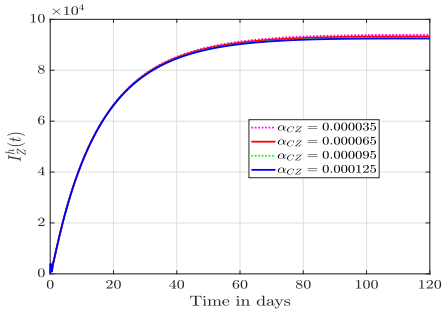

(a) Varying effective contact rate for co-infection transmission on infectious humans with Zika.

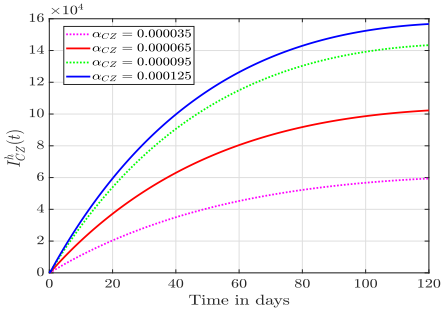

(b) Varying effective contact rate for co-infection transmission on co-infection.

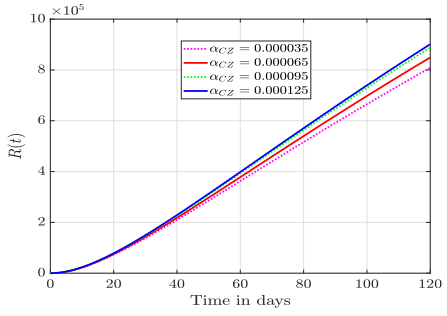

(c) Varying effective contact rate for co-infection transmission on recovered humans.

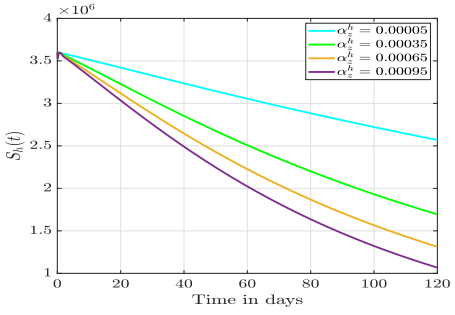

(d) Varying the effective contact rate for human-vector transmission of Zika on susceptible humans.

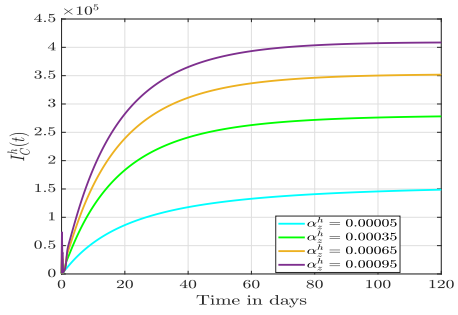

(e) Varying the effective contact rate for human-vector transmission of Zika on infectious humans with COVID-19.

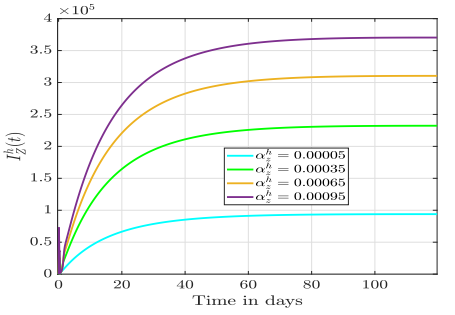

(f) Varying the effective contact rate for human-vector transmission of Zika on infectious humans with Zika.

Fig. 7. Numerical simulation under hybrid derivative with fractal-fractional order of 0.99.

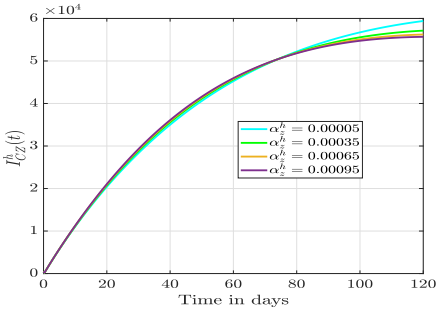

(a) Varying the effective contact rate for human-vector transmission of Zika on co-infection with COVID-19 and Zika.

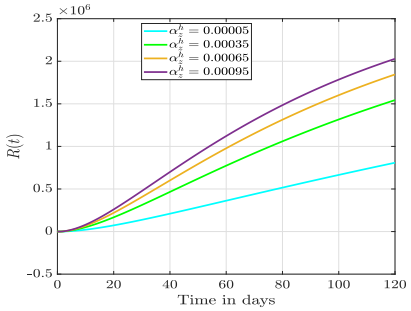

(b) Varying the effective contact rate for human-vector transmission of Zika on recovered humans.

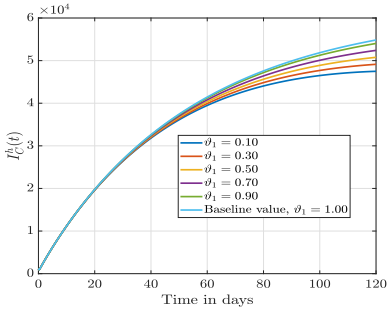

(c) The effects of varying the re-infection rate on infectious humans with COVID-19.

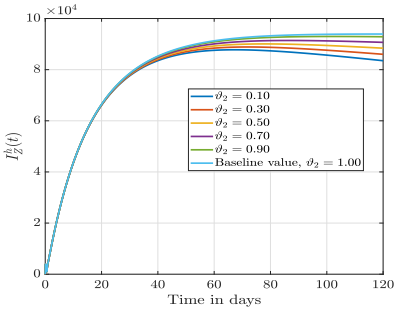

(d) The effects of varying the re-infection rate on infectious humans with Zika.

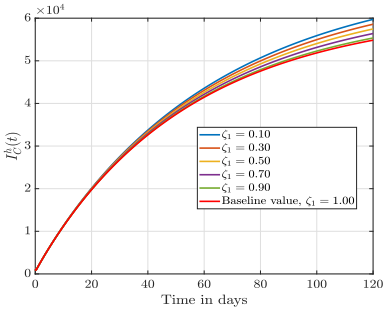

(e) Effects of varying the modification parameter on infectious humans with COVID-19.

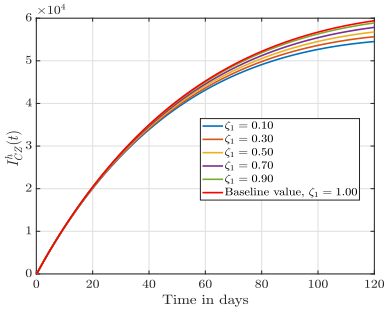

(f) Effects of varying the modification parameter on humans co-infected with COVID- 19 and Zika virus.

Fig. 8. Numerical simulation under hybrid derivative with fractal-fractional order of 0.99.

References

[1] Vicente CR, da Silva TCC, Pereira LDA, Miranda AE. Impact of concurrent epidemics of dengue, Chikungunya, Zika, and COVID-19. Rev Soc Bras Med Trop 2021;54:e08372020.

[2] McBroom KA. Comparison of Zika virus and COVID-19: Clinical overview and public health messaging. J Midwifery Women's Health 2021;66(3):334–42.

[3] Beigi RH. Emerging infectious diseases in pregnancy. Obstet Gynecol 2017;129(5):896–906.

[4] Ali S, Gugliemini O, Harber S, et al. Environmental and social change drive the explosive emergence of Zika virus in the Americas. PLoS Negl Trop Dis 2017;11(2):e0005135.

[5] Grubaugh ND, Saraf S, Gangavarapu K, et al. Travel surveillance and genomics uncover a hidden Zika outbreak during the waning epidemic. Cell 2019;178(5):1057–71.e11.

[6] Centers for disease control and prevention. Zika in the US. Centers for Disease Control and Prevention website; 2019, https://www.cdc.gov/zika/geo/index.html. [Accessed 20 October 2020].

[7] World Health Organization. Infant feeding in areas of Zika virus transmission. In: E-library of evidence for nutrition actions. World Health Organization; 2019, https://www.who.int/elena/titles/zikabreastfeeding/en/. [Accessed 1 March 2021].

[8] WHO Coronavirus (COVID-19) dashboard. 2022, https://covid19.who.int/. [Accessed 6 June 2022].

[9] Omame A, Nwajeri UK, Abbas M, Onyenegecha CP. A fractional order control model for diabetes and COVID-19 co-dynamics with Mittag-Leffler function. Alex Eng J 2022;61(10):7619–35.

[10] Omame A, Rwezaura H, Diagne ML, Inyama SC, Tchuenche JM. COVID-19 and dengue co-infection in Brazil: Optimal control and cost-effectiveness analysis. Eur Phys J Plus 2021;136(10):1090.

[11] Omame A, Okuonghae D, Nwafor UE, Odionyenma BU. A co-infection model for HPV and syphilis with optimal control and cost-effectiveness analysis. Int J Biomath 2021;14(07):2150050.

[12] Kumar P, Erturk VS, Almusawa H. Mathematical structure of Mosaic disease using microbial biostimulants via Caputo and Atangana-Baleanu derivatives. Res Phys 2021;24:104186.

[13] Mohammadi H, Kumar S, Rezapour S, Etemad S. A theoretical study of the Caputo–Fabrizio fractional modeling for hearing loss due to Mumps virus with optimal control. Chaos Solitons Fractals 2021;144:110668.

[14] Alshehri HM, Khan A. A fractional order hepatitis C mathematical model with Mittag-Leffler kernel. J Funct Spaces 2021;2021:2524027.

[15] Rezapour S, Etemad S, Mohammadi H. A mathematical analysis of a system of Caputo–Fabrizio fractional differential equationsfor the anthrax disease model in animals. Adv Differ Equ 2020;2020:481.

[16] Kumar P, Erturk VS. Environmental persistence influences infection dynamics for a butterfly pathogen via new generalised Caputo type fractional derivative. Chaos Solitons Fractals 2021;144:110672.

[17] Kumar P, Erturk VS, Yusuf A, Nisar KS, Abdelwahab SF. A study on canine distemper virus (CDV) and rabies epidemics in the red fox population via fractional derivatives. Res Phys 2021;25:104281.

[18] Baleanu D, Etemad S, Rezapour S. A hybrid Caputo fractional modeling for thermostat with hybrid boundary value conditions. Bound Value Probl 2020;2020:64.

[19] Thaiprayoon C, Sudsutad W, Alzabut J, Etemad S, Rezapour S. On the qualitative analysis of the fractional boundary value problem describing thermostat control model via ψ-Hilfer fractional operator. Adv Differ Equ 2021;2021:201.
[20] Rezapour S, Tellab B, Deressa CT, Etemad S, Nonlaopon K. H-U-type stability and numerical solutions for a nonlinear model of the coupled systems of Navier BVPs via the generalized differential transform method. Fractal Fract 2021;5(4):166.
[21] Wang Y, Xiao J. A Liouville problem for the stationary fractional Navier–Stokes–Poisson system. J Math Fluid Mech 2018;20:485–98.
[22] Alzabut J, Selvam GM, El-Nabulsi RA, Vignesh D, Samei ME. Asymptotic stability of nonlinear discrete fractionalpantograph equations with non-local initial conditions. Symmetry 2021;13:473.
[23] Wongcharoen A, Ntouyas SK, Tariboon J. Nonlocal boundary value problems for Hilfer type pantograph fractional differentialequations and inclusions. Adv Differ Equ 2020;2020:279.
[24] Zhang L, Addai E, Ackora-Prah J, Arthur YD, Asamoah JKK. Fractional-order Ebola-Malaria coinfection model with a focus on detection and treatment rate. Comput Math Methods Med 2022.
[25] Adu IK, Wireko FA, Sebil C, Asamoah JKK. A fractal–fractional model of Ebola with reinfection. Results Phys 2023;52:106893.
[26] Addai E, Zhang L, Ackora-Prah J, Gordon JF, Asamoah JKK, Essel JF. Fractal-fractional order dynamics and numerical simulations of a Zika epidemic model with insecticide-treated nets. Physica A 2022;603:127809.
[27] Addai E, Zhang L, Asamoah JKK, Preko AK, Arthur YD. Fractal–fractional age-structure study of omicron SARS-CoV-2 variant transmission dynamics. Part Diff Equ Appl Math 2022;6:100455.
[28] Rezapour S, Asamoah JKK, Hussain A, Ahmad H, Banerjee R, Etemad S, et al. A theoretical and numerical analysis of a fractal–fractional two-strain model of meningitis. Results Phys 2022;39:105775.
[29] Ackora-Prah J, Seidu B, Okyere E, Asamoah KKJ. Fractal–fractional Caputo Maize streak virus disease model. Fractal Fract 2023;7(2):189.
[30] Asamoah JKK, Fatmawati. A fractional mathematical model of heartwater transmission dynamics considering nymph and adult amblyomma ticks. Chaos Solitons Fractals 2023;174:113905.
[31] Asamoah JKK, Sun GQ. Fractional Caputo and sensitivity heat map for a gonorrhea transmission model in a sex structured population. Chaos Solitons Fractals 2023;175:114026.
[32] Wireko FA, Adu IK, Sebil C, Asamoah JKK. A fractal–fractional order model for exploring the dynamics of Monkeypox disease. Decis Anal J 2023;8:100300.
[33] Adom-Konadu A, Bonyah E, Sackitey AL, Anokye M, Asamoah JKK. A fractional order Monkeypox model with protected travelers using the fixed point theorem and Newton polynomial interpolation. Healthcare Anal 2023;3:100191.
[34] Nwajeri UK, Asamoah JKK, Ugochukwu NR, Omame A, Jin Z. A mathematical model of corruption dynamics endowed with fractal–fractional derivative. Results Phys 2023;52:106894.
[35] Bonyah E, Khan MA, Okosun KO, Gomez-Aguilar JF. On the co-infection of dengue fever and Zika virus. Optim Control Appl Meth 2019;40(3):394–421.
[36] Omame A, Abbas M, Onyenegecha CP. A fractional-order model for COVID-19 and tuberculosis co-infection using Atangana-Baleanu derivative. Chaos Solitons Fractals 2021;153:111486.
[37] Nwankwo A, Okuonghae D. Mathematical analysis of the transmission dynamics of HIV syphilis co-infection in the presence of treatment for syphilis. Bull Math Biol 2018;80(3):437–92.
[38] Omame A, Isah ME, Abbas M, Abdel-Aty AH, Onyenegecha CP. A fractional order model for dual variants of COVID-19 and HIV co-infection via Atangana-Baleanu derivative. Alex Eng J 2022;61(12):9715–31.
[39] Omame A, Abbas M, Onyenegecha CP. A fractional order model for the co-interaction of COVID-19 and Hepatitis B virus. Results Phys 2022;37:105498.
[40] Atangana A. Fractal-fractional differentiation and integration: Connecting fractal calculus and fractional calculus to predict complex system. Chaos Solitons Fractals 2017;102:396–406.
[41] Owolabi KM, Atangana A, Akgul A. Modelling and analysis of fractal-fractional partial differential equations: Application to reaction–diffusion model. Alex Eng J 2020;59(4):2477–90.
[42] Atangana A, Qureshi S. Modeling attractors of chaotic dynamical systems with fractal-fractional operators. Chaos Solitons Fractals 2019;123:320–37.
[43] Atangana A, Araz SI. New numerical approximation for Chua attractor with fractional and fractal-fractional operators. Alex Eng J 2020;59(5):3275–96.
[44] Atangana A, Araz SI. New numerical scheme with newton polynomial: theory, methods, and applications. Academic Press; 2021.
[45] Atangana A, Araz SI. A novel Covid-19 model with fractional differential operators with singular and non-singular kernels: Analysis and numerical scheme based on Newton polynomial. Alex Eng J 2021;60(4):3781–806.
[46] Asamoah JKK. Fractal-fractional model and numerical scheme based on Newton polynomial for Q fever disease under Atangana-Baleanu derivative. Res Phys 2022;34:105189.
[47] Shah K, Arfan M, Mahariq I, Ahmadian A, Salahshour S, Ferrara M. Fractal-fractional mathematical model addressing the situation of Corona virus in Pakistan. Res Phys 2020;19:103560.
[48] Gomez-Aguilar JF, Cordova-Fraga T, Abdeljawad T, Khan A, Khan H. Analysis of fractal-fractional malaria transmission model. Fractals 2020;28(8):2040041.
[49] Ali Z, Rabiei F, Shah K, Khodadadi T. Qualitative analysis of fractal-fractional order COVID-19 mathematical model with case study of Wuhan. Alex Eng J 2021;60(1):477–89.
[50] Najafi H, Etemad S, Patanarapeelert N, Asamoah JKK, Rezapour S, Sitthiwirattham T. A study on dynamics of CD4$^+$ T-cells under the effect of HIV-1 infection based on a mathematical fractal-fractional model via the Adams–Bashforth scheme and Newton polynomials. Mathematics 2022;10(9):1366.
[51] Khan H, Alam K, Gulzar H, Etemad S, Rezapour S. A case study of fractal-fractional tuberculosis model in China: Existence and stability theories along with numerical simulations. Math Comput Simul 2022;198:455–73.
[52] Alqhtani M, Saad KM. Fractal-fractional Michaelis–Menten enzymatic reaction model via different kernels. Fractal Fract 2022;6(1):13.
[53] Farman M, Akgul A, Nisar KS, Ahmad D, Ahmad A, Kamangar S, et al. Epidemiological analysis of fractional order COVID-19 model with Mittag-Leffler kernel. AIMS Math 2022;7(1):756–83.
[54] Saad KM, Alqhtani M, Gomez-Aguilar JF. Fractal-fractional study of the hepatitis C virus infection model. Res Phys 2020;19:103555.
[55] Atangana A, Baleanu D. New fractional derivatives with non-local and non-singular kernel: Theory and applications to heat transfer model. Therm Sci 2016;20:763–9.
[56] Khan MA, Iqbal N, Khan Y, Alzahrani E. A biological mathematical model of vector-host disease with saturated treatment function and optimal control strategies. Math Biosci Eng 2020;17(4):3972–97.
[57] Olaniyi S. Dynamics of Zika virus model with nonlinear incidence and optimal control strategies. Appl Math Inf Sci 2018;12(5):969–82.
[58] Abidemi A, Owolabi KM, Pindza E. Modelling the transmission dynamics of Lassa fever with nonlinear incidence rate and vertical transmission. Phys A: Stat Mech Appl 2022;597:127259.
[59] Ozair M, Lashari AA, Jung IH, Okosun KO. Stability analysis and optimal control of a vector-borne disease with nonlinear incidence. Discr Dyn Nat Soc 2012;2012:595487.
[60] Okuneye KO, Velasco-Hernandez JX, Gumel AB. The unholy Chikungunya-Dengue-Zika trinity: A theoretical analysis. J Biolog Syst 2017;25(04):545–85.
[61] van den Driessche P, Watmough J. Reproduction numbers and sub-threshold endemic equilibria for compartmental models of disease transmission. Math Biosci 2002;180(1–2):29–48.
[62] Granas A, Dugundji J. Fixed point theory. New York: Springer-Verlag; 2003.
[63] https://www.citypopulation.de/en/brazil/cities/espiritosanto/. [Accessed 1 Jan 2022].
[64] Garba SM, Gumel AB, Abu Bakar MR. Backward bifurcations in dengue transmission dynamics. Math Biosci 2008;215(1):11–25.
[65] https://www.indexmundi.com/brazil/demographics_profile.html. [Accessed 1 Jan 2022].